CHAPTER 1

Methods of Visualisation

G. VERHOEVEN[a,b]

[a] Ludwig Boltzmann Gesellschaft GmbH, LBI for Archaeological Prospection and Virtual Archaeology, Franz-Klein-Gasse 1, Wien, 1190, Austria; [b] Ghent University, Department of Archaeology, Sint-Pietersnieuwstraat 35 (110-016), Gent, 9000, Belgium
E-mail: Geert.Verhoeven@Archpro.lbg.ac.at

1.1 Introduction

In the fields of cultural heritage, archaeology, art history and museology, many examination methods are based on imaging techniques. To date, numerous different imaging approaches exist, and although most of them have already existed for several decades, recent advantages in hard- and software technology make their application more straightforward than ever. In this chapter, an elementary but essential coverage of photodetectors, illumination equipment and signal composition will be provided to better understand the basic principles of common non-destructive scientific visualisations such as broadband colour photography, non-visible ultraviolet and infrared imaging, fluorescent photography, spectral imaging and X-ray radiography. Although important, many means to characterise and depict archaeological and heritage object will not be discussed (such as particle induced X-ray emission or PIXE, ultrasound techniques, thermography, stereomicroscopy, computed tomography, neutron imaging), nor will the file formats needed to store these visualisations and many other related archiving issues. For those interested in these topics, the following chapters of this book and the excellent compendium of MacDonald[1] are recommended. Although several practical examples will illustrate each and every visualisation technique tackled in this chapter, it is still necessary to go back to some

Analytical Archaeometry: Selected Topics
Edited by Howell Edwards and Peter Vandenabeele

Published by the Royal Society of Chemistry, www.rsc.org

basic physics. Since imaging art objects and archaeological artefacts are all based upon some essential principles of how matter interacts with radiant energy, this chapter will start with a concise exploration of the world of matter, charge and energy.

1.1.1 Electromagnetic Radiation

Matter can be described as anything that occupies space and has weight. It is constituted by elements in various combinations. These elements, all described in the periodic table, are made up of atoms. Such atoms can be seen as the smallest matter particle, retaining all physical characteristics of an element. Different atom models were proposed during the last two centuries. Today, the Bohr model—introduced by Niels Bohr in 1913—is often used, as it offers an easy way to depict the atom besides a relative correctness. In this model, the central core or nucleus of the atom is made up of chargeless neutrons and positively charged protons, whose amount is indicated by the atomic number Z. To compensate for these positive charges, negatively charged particles or electrons orbit this nucleus. Hence, it is correct to say that electric charge is substance-like and that all physical objects are composed of electric charge.

Charge differs from energy. Energy should not be looked at as a substance but rather as an attribute of a system that always turns out to be conserved. To be able to track energy flows, energy can be conceptualised by the model of fields. In the same way that a massive object can produce a gravity field to which distant objects respond, electrical charges and magnets alter the region of space around them so that they can exert forces on distant objects. It is exactly this altered space that is called a *field* (more technically, these fields are just vector quantities). Scientists have known since the early part of the 19th century that electrical fields and magnetic fields are intimately related to each other: moving electric charges (*i.e.* electric current) create a magnetic field and a changing magnetic field creates electrical current (thus electrical fields). A consequence of this is that changing electric and magnetic fields should trigger each other. The Scottish mathematician and physicist James Clerk Maxwell (1831–1879) put these ideas together and mathematically described the relationship between the magnetic and electric fields, as well as the currents and charges that create them. To conclude this line of reasoning, Maxwell said that visible light is an electromagnetic (EM) wave, consisting of both an electric (**E**) and magnetic (**B**) field (Figure 1.1). Both fields are oscillating perpendicular to each other as well as perpendicular to the direction of propagation (which makes them a transverse wave), whilst propagating at 299 792 458 m s^{-1} in vacuum. The latter speed is known as the speed of light, denoted c, and decreases when light travels in air, glass, water or other transparent substances.[2–4]

The electric and magnetic component vectors vibrate in phase and are sinusoidal in nature: they oscillate in a periodic fashion as they propagate

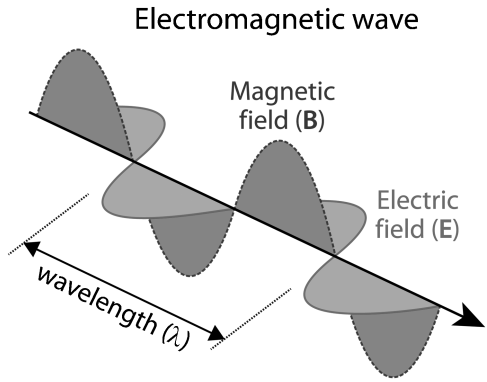

Figure 1.1 An electromagnetic (EM) wave consisting of electric and magnetic oscillating fields. In this example, the oscillating magnetic field vectors are indicated with a dotted line.

through space and have peaks and troughs (see Figure 1.1). Being a self-propagating and periodic wave-like phenomenon, EM radiation is distinguished by the length of its waves, called the wavelength (λ), its magnitude of change or amplitude (A) as well as its frequency (v): a figure—expressed in Hertz (Hz)—that indicates the number of complete waves or sinusoidal cycles passing a certain point in one second and thus inversely proportional to λ. No matter what portion of this broad spectrum is considered, they all obey the same physical laws and the relation $c = \lambda v$ holds for each.

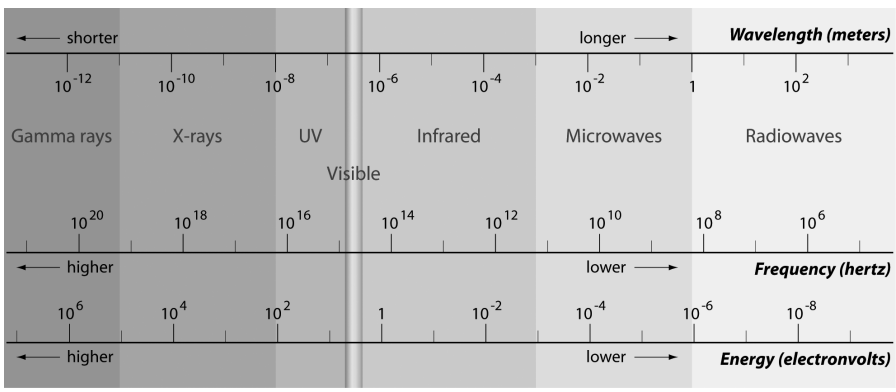

Figure 1.2 The EM spectrum.

1.1.2 Light and Beyond-visible Radiation

The principle that allows the human visual system to observe objects and persons is based on those subjects' reflection of visible light. Dark objects do not reflect much incoming light, whereas a healthy banana principally reflects yellow light. However, this light is only one small portion out of the complete, so-called EM spectrum radiated by the sun or other sources (like stars or lamps). The EM spectrum can be considered a continuum of varying EM waves, all consisting of electric and magnetic fields that are described by the Maxwellian theory, but distinguishable by their wavelength.

Visible light (''light''), for instance, is only a very narrow spectral band with wavelengths ranging from approximately 400 nm (400×10^{-9} m) to 700 nm (700×10^{-9} m), the absolute thresholds varying from person to person and specific viewing conditions. These wavelengths correspond with frequencies comprised between 7.49×10^{14} Hz (749 THz) to 4.28×10^{14} Hz (428 THz). Nonetheless, the complete EM spectrum consists of far more particular wavebands with characteristic frequencies and related wavelengths that are not perceivable by the unaided normal human eye. To both sides of the visible band there is EM radiation which does not produce a visual sensation: gamma rays, X-rays, and ultraviolet (UV) rays with shorter-than-visible wavelengths (and higher frequencies), while infrared (IR) rays, microwaves, and radiowaves can be found in the long-wavelength, low-frequency region (Figure 1.2).

In addition to the aforementioned wave properties, EM radiant energy is known to exhibit particle-like behaviour and can be seen as a travelling bundle of photons (*i.e.* discrete energy packets) with energy levels that differ according to the wavelength. EM radiation can thus be considered a vehicle for transporting energy from the radiation source to a destination, photons being the particles of EM energy. To calculate a photon's quantum energy (E), Planck's constant h (*i.e.* 6.626×10^{-34} J s^{-1} or 4.136×10^{-15} eV s^{-1}) must be multiplied by the frequency v of the radiation.

Due to this quantization, a visible photon with a wavelength of 650 nm will always have 1.9 eV of energy, while an ultraviolet 345 nm wavelength is characterised by photons with quantum energies of 3.6 eV. From these figures, it is obvious that shorter wavelengths have higher radiative energies (see also Figure 1.2). None of the wave-like and particle-like descriptions is complete by itself, but each of them a valid description of some aspects of EM radiation behaviour. This wave–particle duality is still one of the key concepts in quantum mechanics.[2–4]

This chapter will be mainly restricted to imaging in the *optical radiation spectrum*. Although the limits (and also the number of subdivisions) are to a certain extent dependent on the discipline dealing with EM radiation and hence largely varying through literature, it is commonly accepted that the optical spectral band reaches from the UV to the IR. Since the subdivisions in one spectral band are not unified amongst various sciences, one finds several outer limits for the optical radiation spectrum. As was also defined by Palmer

	Division	Subdivision	Abbreviation	Cut-on (nm)	Cut-off (nm)
Optical radiation	UltraViolet (UV)	Vacuum UV	VUV / UV-D*	10	200
		Far UV	FUV / UV-C*	200	280
		Middle-UV	MUV / UV-B	280	315
		Near-UV	NUV / UV-A	315	400
	Visible (Vis)	Blue	B	400	500
		Green	G	500	600
		Red	R	600	700
	InfraRed (IR)	Near-IR	NIR	700	1100
		Short Wavelength IR	SWIR	1100	3000
		Mid Wavelength IR	MWIR	3000	6000
		Long Wavelength IR	LWIR	6000	15000
		Far/Extreme-IR	FIR	15000	1000000

Figure 1.3 The divisions of the optical EM radiation (* VUV does not perfectly correspond to UV-D. While VUV runs from 10 nm to 200 nm and FUV from 200 nm to 280 nm, UV-D encompasses the 10 nm to 100 nm region and UV-C the 100–280 nm zone).

and Grant[5] and Ohno,[6] optical radiation is here defined as EM waves with wavelengths between 10 nm (0.01 μm) to 1 mm (1000 μm). In this way, it exactly covers a five-decade frequency range from 3×10^{11} Hz to 3×10^{16} Hz and can be logically subdivided into various spectral bands (Figure 1.3). The designation of spectral sub-ranges also varies, with the largest variability in the infrared band (even in the same discipline). Often, one finds NIR (see Figure 1.3 for abbreviations) to end at 1400 nm and SWIR finishing at 2500 nm. Additionally, the visible and NIR range are often referred to as the VNIR band. In the UV region, there is slightly more agreement, although UV-D is sometimes not considered to be part of the optical radiation spectrum.

Both the UV and IR region have the advantage that they can convey information about an object that remains unnoticed by the human eye. In this chapter, the optical radiation under consideration will be restricted to the NUV-SWIR wavelengths, as this is the most common spectral region used in (heritage) imaging. However, the final part of this chapter will delve a bit deeper in the X-ray region. While X-rays do not belong to the optical band of EM radiation, they have been used for over a century as a diagnostic tool in cultural heritage imaging. As such, X-ray radiography completes the triad of imaging phenomena outside the visible light that will be tackled here. Before delving deeper into these topics, it is useful to look more closely at the possible detectors for optical radiation and create a broader understanding of the terms signal and noise.

1.2 Detecting and Imaging Optical Radiation

1.2.1 Principles

Imaging a medium is always dependent on the influence of matter on incident EM radiation, which involves processes such as refraction, polarization change, specular reflection, scattering and absorbance.[7] In a simplified form: the surface of any natural and synthetic object transmits, reflects, and absorbs EM radiation in varying ratios. Besides the specific chemical and physical structure of the object, this interaction and particular ratio of the three processes is wavelength dependent.[8] The reflectance of an object can thus be described as the ratio of all the energy reflected (or scattered) by the surface *versus* the total amount of incident energy. When defined per unit wavelength, reflectance is termed spectral reflectance. A medium-specific *spectral signature/spectral reflectance curve/spectral reflectance distribution* is yielded when the spectral reflectance is plotted over a specific spectral range (see Figure 1.4). Recording this spectral signature not only tells us what colour an object has, but can also give insight into its chemical composition, since the heterogeneity of diverse elements in an object gives rise to different matter–radiation interactions and creates contrast in an image. However, detecting and imaging such a reflectance spectrum is not that straightforward, since imaging optical

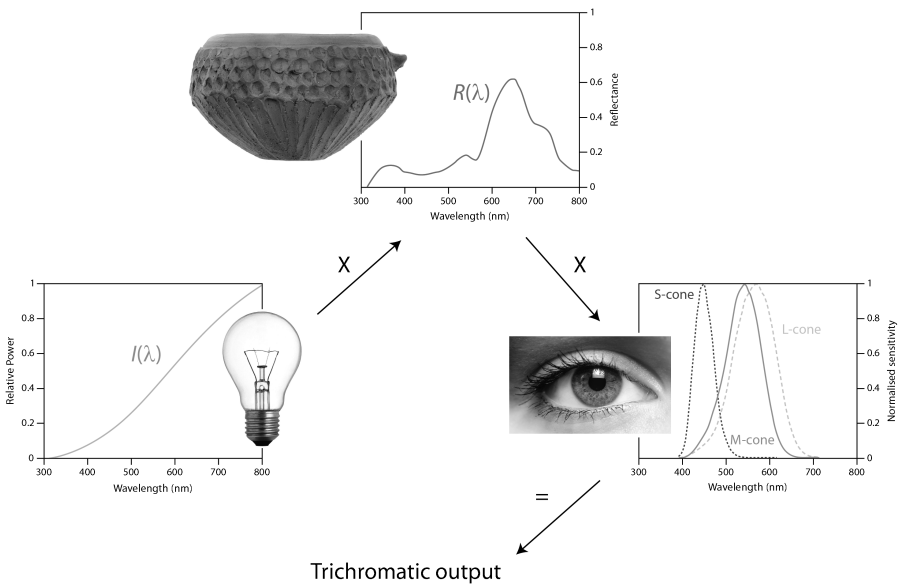

Figure 1.4 The trichromatic output generated by the human visual system or any RGB camera results from two multiplications. First, the spectral power distribution $I(\lambda)$ of the radiation source interacts with the spectral reflectance $R(\lambda)$ of the object. This stimulus is subsequently integrated over the cone response curves (or the RGB curves of the digital camera) and creates a trichromatic signal.

radiation involves in many cases a multiplicative effect: only the portion of the incoming radiation that is reflected by the object will be imaged (Figure 1.4).

This shows why human vision, colour photography or any kind of optical digital imaging (except fluorescence and thermal imaging in which only the emitted EM radiation is recorded) generates a signal that is the outcome of a three-variable process. First, there is the radiation source which has a certain spectral power distribution $I(\lambda)$: *i.e.* a certain "amount " of radiation emitted at each wavelength. Secondly, the object itself has certain reflection properties which will vary per wavelength: $R(\lambda)$. The combination of both incoming EM energy and reflection $[I(\lambda) \times R(\lambda)]$ creates a spectral distribution $\phi(\lambda)$ that is sampled by the human eye or the digital imaging sensor. Those also have their own spectral response; they will absorb the photons in specific spectral regions and interpret them. To make things even more complicated, also the viewing and illumination geometry matter, although these will be omitted in this chapter. When one of those three parameters changes, the visual sensation or the pixel values in the digital image will differ.

In the next session, a short overview will be presented on sensors commonly used for optical imaging.

1.2.2 Photodetectors

1.2.2.1 The Human Visual System

A very important and certainly the most familiar detector of optical radiation is the human eye and brain, together forming the human visual system. To enable vision under dim lighting conditions (*scotopic vision*), about 100 million very light-sensitive rods are used. Since rods only send information about the quantity of light, night vision is said to be colour-blind.[9,10] When the light becomes more intense (from bright moonlight up), the rods gradually stop functioning as they get saturated. More importantly, colours will appear as the five to six million cones come into play: *i.e. photopic vision*.[9,10] Most humans have three cone variants with a specific response to visible wavelengths (Figure 1.4): short-, middle-, and long-wavelength sensitive cones (S, M, and L), named according to the part of the visible spectrum to which they are most sensitive and characterised by peak sensitivities λ_{max} at about 445 nm, 540 nm, and 565 nm respectively.[11] Due to its working principle based on three different cone types, the human colour vision is said to be trichromatic.[10] Figure 1.4 shows that the three receptors have a quite broad waveband to which they respond and there is significant overlap between the three responses.

When the eye captures incoming light, it is integrated over three broad bands and transformed into a mix of three signals (one for every individual detector) and processed by the brain. As a result, individual persons with a normal vision will see the same objects with slightly different colours, since the cone responses show some variation amongst humans. Additionally, objects with

different spectral characteristics can produce identical cone responses, hence representing the same colour. Such spectra are called *metamers* and the effect is known as *metamerism*.[10,12,13] Since metamerism can be defined as the production of equal spectrally-integrated responses from dissimilar spectral signals, an imaging system with only one, two or three spectral channels is said to be a metameric imaging system.[13,14] Monochrome image sensors and conventional digital cameras will create metameric images since these imagers will produce identical integrated outputs from a variety of incoming spectral power distributions. Due to this behaviour, spectral imaging using at least four spectral bands is needed to overcome the limits of metameric imaging and tell whether a different image signal is the result from a change in illumination or object properties. The following sections will provide more info on this topic, but not before looking at the some widespread means to digitally detect optical radiation.

1.2.2.2 Digital Photodetectors

To date, detecting optical radiation is usually accomplished by the conversion of incoming EM radiation into an electrical output signal which is then digitised. Most digital image capture systems comprise optical elements such as lenses, mirrors, prisms, gratings and filters that gather the radiation and focus it onto an imaging sensor. This imaging sensor itself consists of one or more optical detectors (also called *photodetector*) that can detect the incoming radiation and generate a signal in response to that EM radiation. Most imaging sensors are *focal plane arrays* (FPAs), since they consist of an assemblage of individual photodetectors located at the focal plane of the imaging system.

During the last decennium, many technologies were developed to make the detection of optical radiation possible. In the 1920s and 1930s, there was the flourishing technology of vacuum tube sensors which culminated in the advent of television.[15] A major breakthrough was achieved in 1969, when the charge-coupled device (CCD) was invented at AT&T Bell Labs by Willard Boyle and George E. Smith.[16] Forty years later, the CCD is still around and developed into a major digital imaging technology that is nowadays still used in various professional and scientific applications in need for high-quality image data, mainly in the visible and near-infrared (NIR) spectrum. One of the most well-known examples of recent history is most likely the CCD-based camera on-board the Hubble space telescope. Although CCDs have always been able to perform very efficiently and uniformly over large areas, the serial access to the image data, the power consumption and the required high charge transfer efficiency were limitations difficult to overcome.[17] In the early 1990s, Eric Fossum led a team at NASA's Jet Propulsion Lab (JPL) that came up in 1993 with the CMOS APS (complementary metal oxide semiconductor active pixel sensors) technology as a way to overcome these issues and reduce the size of cameras launched on spacecrafts.[18,19] In the late 1990s and 2000s, further

improvements of the these CMOS APS imagers were achieved, mostly driven by the cell phone market that needed cheaper and smaller imagers on top of a lower power consumption and better integration. *Anno* 2012, both CMOS and CCD imagers have the potential to deliver a very high-quality image output with costs that are quite similar.[20] However, both have specific advantages and drawbacks that explain why currently CMOS sensors are dominating the photographic market (smaller, less power consumption, greater data throughput) and CCDs are king in the very high-quality scientific imaging for astronomy or for high-resolution digital camera backs (low noise, uniformity, linearity, near-theoretical sensitivity). Both CCDs and CMOS imagers have silicon (Si, $Z = 14$) as their basis and can detect radiation to about 1100 nm (the so-called cut-off wavelength). Longer wavelength radiation has photons whose energy is too small to create a response in the detector.[21] Although different manufacturing processes can be used, the general useful spectral response of CCDs and CMOS imagers is situated from the NUV (around 320–370 nm) to 1100 nm (the limit of NIR).

For detection in the other EM bands, other sensor types and materials are necessary. To simplify the comparison of different optical detectors, the detectivity D^* (called *D-star*) was defined.[15,22] In Figure 5A, the D^* of several photodetectors is plotted as a function of wavelength. Note that D^* must be high to detect low irradiance levels. Figure 6B displays the spectral quantum efficiency (QE or percentage of incident photons that will effectively be used to build up the final signal) of various detector materials applied to create arrays for UV, visible and IR sensing. From both graphs, it is obvious that the detector material of choice for imaging in the NIR and first part of the SWIR is the semiconductor InGaAS (Indium Gallium Arsenide). InGaAS photodetectors are semiconductors composed of indium, gallium and arsenic that have a high QE in the 900 nm (0.9 μm) to 1.68 μm range. However, InGaAs detectors with a longer wavelength cut-off are also produced and operate in the 0.9 μm to 2.55 μm spectral range.[23,24] This means that InGaAS detectors really start to shine where silicon CCD and CMOS imagers begin to leave off. Because of their low-cost, lead oxide-lead sulfide (PbO-PbS) vidicons often have been applied for hyperspectral imaging of paintings and drawings (see later) in the visible to SWIR range, although their resolving power and sensitivity is nowadays regarded as very low.[25] Many other infrared technologies exist as well, all of them sensitive to a specific portion of the broad infrared spectrum and consisting of several materials. Germanium (Ge) is for instance used in the NIR, whereas indium antimonide (InSb), platinum silicide (PtSi), indium arsenide (InAs), mercury cadmium telluride (HgCdTe) and germanium doped with copper (Cu) and gold (Au) in the longer IR wavebands.

Although the individual silicon photodiode detector might have a decent blue and NUV response (at room temperature 320 nm for the normal photodiode), the spectral sensitivity curve of a CCD or CMOS imaging sensor significantly drops after 450 nm since the electrodes and oxide coatings in the

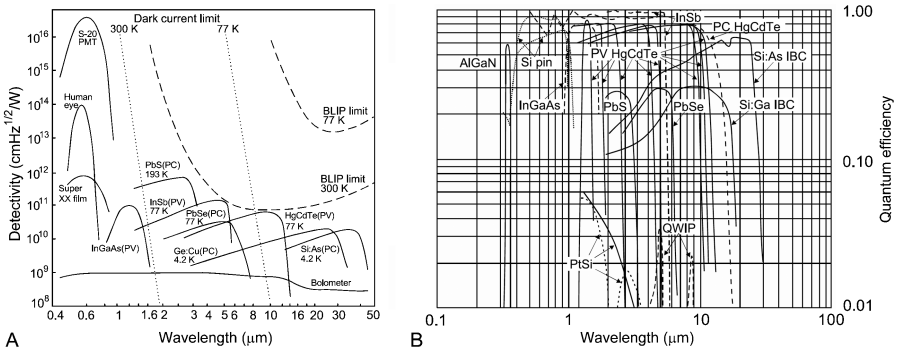

Figure 1.5 (A) Detectivity D^* as a function of wavelength for various photodetectors. PC, PV and PMT indicate the detector type, respectively photoconductive detector, photovoltaic detector and photomultiplier tube; (B) the QE of UV, visible and IR detector arrays. (Reproduced with permission from ref. 15)

sensor's surface layers absorb the short visible wavelengths.[26] Luckily, there exist several methods for enhancing CCD and CMOS sensors for UV imaging applications (such as phosphor coating or backside thinning/illuminating). Nowadays, scientific back-side illuminated silicon CMOS and CCD imagers allow deep UV imaging down to 200 nm.[27]

1.2.3 Signals and Noise

Digital photodetectors generate digital numbers (DNs). However, these DNs are made of several particular contributions. By unravelling all the components that add to the final DN, it will afterwards be possible to untangle the whole process and think about the necessary steps to extract the only component of interest. In scientific digital imaging, only the stream of photons that reach the sensor (*i.e.* the photon signal) is of interest. However, the *radiance frame*/*raw image* S_{raw} (sometimes called light frame) produced by an image sensor is not only produced by the incident photons. Generally, the raw image consists of three particular constituents:[28,29]

- the *photon signal*, which is generated by the accumulated EM radiation during the exposure;
- the *dark current signal* that is produced by thermally induced electrons, even when the sensor is not illuminated. This signal accumulates with integration time (exposure) and is temperature dependent;
- the *bias signal*/*DC offset*, a small and mostly steady zero voltage offset generated due to the effects of electrical charge applied to the detector prior to exposure. Also this signal occurs in the total absence of illumination.

Each of these non-random signals has some corresponding *noise* embedded, in which noise is defined as the *unavoidable random deviations from the nominal*

signal values. These noise sources, which are always present to a certain extent when detecting optical energy, interfere with the photon signal and can bias or even mask this signal. The topic of noise is a complex subject and the noise encountered varies according to the imaging technology used.[30–32] However, almost all images incorporate the following noise:

- **photon/shot/photon shot noise**, caused by the inherently random process of photon arrival; this noise is fundamental, in that it is not correlated with the detector or electronics but results from the detection process itself. This noise obeys the law of Poissonian statistics;
- **dark current (DC)/dark current shot noise**, as with photon noise also caused by the inherently random process of photon arrival and obeying the law of Poissonian statistics;
- **read/readout/bias noise**, a signal independent noise source that is the sum of many components such as reset noise, on- and off-chip amplifier noise and quantization noise.

So, the raw image constituents are the photon signal (with its corresponding Poisson photon noise), an unwanted dark current signal (with Poisson dark current noise) and a bias constant (with readout noise). Any type of noise (or a combination of noise powers) sets an upper limit to the detectivity of a photodetector. The ultimate performance limit for a detector is achieved when the photon noise dominates, since the photon noise is fundamental because it arises from the physical principles of EM radiation detection itself. Many of the imaging processes described later will implement one or several techniques to reduce the amount of noise in the image and try to extract the photon signal. Once a raw image is corrected for the two additive components (dark current and bias) and one multiplicative component (the non-uniform response of the individual photodetectors and illumination of the object) it is termed a *calibrated image* (see Berry and Burnell[28] for all possible calibration steps). Besides those elementary image correction techniques, there are many other post-processing techniques that can be called upon at a specific stage in a particular imaging workflow: examples are white and black point compensation, smoothing, contrast adjustments, image alignment and mosaicking, lens distortion correction and image deconvolution.

In the next sections, we will try to focus on imaging in different parts of the optical electromagnetic spectrum. As this chapter is an introduction to the subject rather than an exhaustive overview, the spectral domains and the imaging tools will be limited to those most commonly used or those that allow getting very decent results with minimal effort and investment. To this end, a great deal of attention will be given to the use of digital single-lens reflex cameras (known as D-SLRs). Because these devices are commercially available, they allow for low-cost, straightforward high-resolution scientific imaging in the NUV, visible and NIR domain. These tools are mainly used to integrate broad spectral regions and give some qualitative information. Afterwards, it will be shown how reflectography changed the way cultural

heritage was visualised in the short wavelength infrared (SWIR) region. Thirdly, the use of industrial imagers for spectral imaging in the same NUV to SWIR domains will be considered. Finally, a short introduction into radiography with non-optical X-rays will be presented.

1.3 RGB D-SLRs for NUV, Visible, Fluorescence and NIR Imaging

1.3.1 D-SLRs

Since the 1990s, much has changed in the photographic world due to the arrival of sophisticated digital still cameras (DSCs) and major advances in computer technology. Unlike video or silver halide photographic cameras, a DSC equals a camera equipped with both a digital image sensor (a silicon CCD or CMOS sensor) for capturing photographs and a storage device for saving the obtained image signals in a digital way.[33] This section will focus on the use of small format digital single-lens reflex cameras (D-SLRs) as they allow switching lenses, which is certainly important for NUV photography. Notwithstanding this constraint, most principles tackled also hold for other DSC formats and most camera types such as compact point-and-shoot DSCs as well as hybrid/bridge/SLR-like camera models.

Whatever the type, almost all D-SLR image sensors consist of a 2D-photosite array to generate a digital photograph. The light-sensitive area of every photosite, in most cases a photodiode or photogate, collects the photons during the exposure time. A digital camera which yields 12.2 million pixels has a sensor built-up by at least 12.2 million photodiodes (*e.g.* 4288 columns x 2848 rows), as one photodiode generally contributes one effective image pixel. On top of this array, manufacturers place a colour filter array (CFA): a mosaic pattern of thin optical filters that are coloured red, green or blue.[30,34] Every individual photosite of the array is covered by such a filter, allowing only one—but broad—particular range of incident radiant energy to be transmitted and subsequently captured by the photodiode (Figure 1.6). As every pixel will initially have one colour component (R or G or B), the other two components get interpolated from neighbouring pixels to create a triplet of integer DNs for every pixel. Generally, small format DSCs use a red-green-blue (RGB) pattern with a repeating group of four photodiodes. When buying a DSC, the imaging sensor is additionally covered with an NUV-NIR blocking/cut-off filter (also called *hot-mirror*) that allows only visible light to pass. By implementing this filter, the camera manufacturer ensures that the sensor's array of photo-sensitive detectors will generate a photographic signal by mainly taking the visible EM radiation into account. This approach is of the utmost importance, as common silicon sensors are inherently sensitive to NUV and especially NIR, whose imaging contribution would be detrimental for image sharpness (since all wavelengths have a different focus), exposure accuracy (DSC light meters are not calibrated for invisible radiation), and true colour reproduction. By

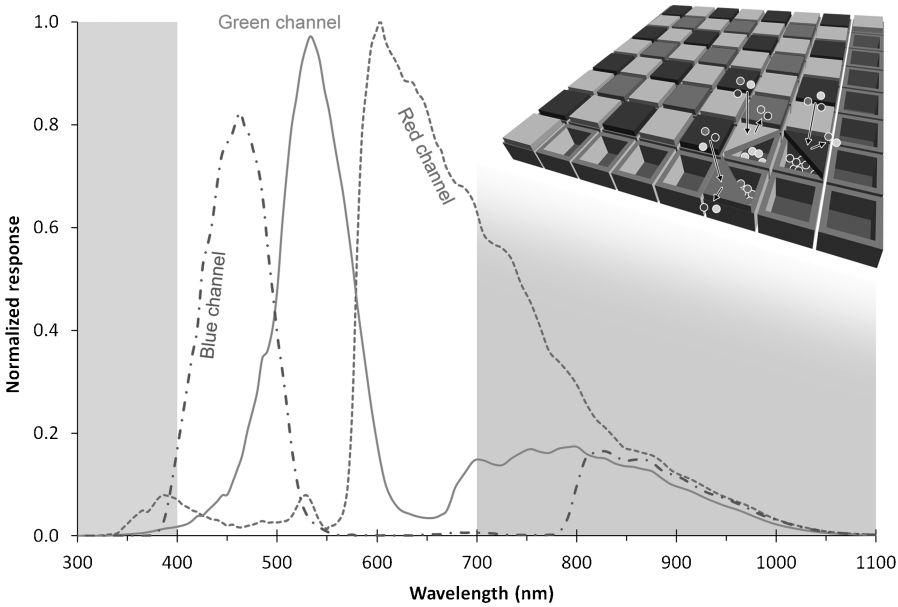

Figure 1.6 The lay-out and working of a typical DSC image sensor with Bayer CFA. The optical filters of the CFA only transmit a broad spectral band of red, green and blue photons. However, the relative spectral response curves obtained from a Nikon D200 without internal hot-mirror reveal that these filters also transmit radiation in the invisible NUV and NIR regions—the latter indicated in grey.

removing this filter, the DSC becomes sensitive to a range of wavelengths exceeding the initial small visible band (Figure 1.6). Because the spectral response of common silicon detectors found in the current DSCs decreases quite rapidly towards shorter wavelengths, the effect of such a modification is most noticeable when imaging the NIR waveband. Notwithstanding, the DSC's responsivity to NUV radiation increases as well, although its sensitivity is far more modest in absolute terms. As was mentioned before, the cut-off wavelength for these imagers is at circa 1100 nm, while the cut-on wavelength can be situated in the 320 nm–370 nm range (for an in-depth overview of sensor sensitivity and DSC modification, see Har[35] and Verhoeven[29,36]).

Although the sensor technology and the specific characteristics of the CFA are responsible for some variation in the spectral responses of DSCs, it is safe to state that Figure 1.6 illustrates the general response one can expect for most CCD and CMOS-based DSCs. Recall that the final camera output is created by the wavelength-dependent reflection of the incoming radiation that gets integrated over the three broad channels. Since the RGB channels are sensitive to light in a large wavelength interval, the RGB values of a pixel (*e.g.* R: 234, G: 121; B: 67) can not be associated to specific wavelengths.[37] Due to this working principle, such three channel imaging systems suffer from the main

drawback of being metameric imagers in which identical integrated RGB outputs can be produced from a variety of dissimilar incoming signals. As a simple example: a metameric imaging system might not be able to distinguish a blue ball illuminated by white light from a white ball illuminated by blue light.

Ideally, DSCs would satisfy the *Luther condition*, which states that any metameric colour-capturing device will create colours that are completely congruent with the colour experience of a human observer if, and only if, its spectral responses mimic the cone sensitivity curves or a linear transformation thereof.[38] The responses of three channel (trichromatic) DSCs are, however, not at all related to the human cone responses because colour accuracy is only one out of several, often mutually exclusive image criteria (such as image noise, low-light sensitivity, resolving power, pleasing colour reproduction, and manufacturing costs) taken into account when designing a DSC.[39,40] In practice, this means that a DSC might generate identical RGB values for two object stimuli which mismatch for the human visual system (and *vice versa*). The metameric DSC matches will thus differ from those of a human observer.[14] Due to this behaviour, DSCs are inaccurate colour reproduction instruments. In contrast, spectral imaging (see later) utilizes a high number of channels to go beyond these restrictions and allow the acquisition of quantitative information such as accurate colour.

1.3.2 Direct Visible Imaging

Many analyses on frescoes and archaeological objects such as vessels and clothing, paintings, ancient manuscripts and any other form of heritage-related content start with a thorough visual examination of the artwork and some visible imaging using ordinary light. To present these artefacts in digital museums or books, conventional images made by reflected visible radiation can be expected to still remain the most important means of visualisation for some years to come. Ideally, these images should be acquired and produced with a high degree of geometrical correctness and colour accuracy. Although the topic of metric accuracy is not considered in this chapter, it has been already indicated that conventional RGB imaging is incapable of achieving the colour accuracy goal completely. However, the examples at the end of this section will prove visible imaging to be useful for many other purposes.

1.3.2.1 Tools

An off-the-shelf DSC is essentially a tool for visible imaging. As the camera will always record spectral information in three distinct spectral bands, a DSC is called a multispectral imaging instrument (although some authors prefer to use the term multispectral only when at least four spectral regions are imaged, just to make the distinction with these conventional DSCs). Besides a wide variety of DSCs with particular possibilities and functions, an amalgam of lenses exists. In such a photographic lens, image formation is achieved by

different optical lens elements, which alter light in different ways. It is the combination of all these elements—usually made of glass—that form the photographic lens and its specific characteristics such as focal length. The interplay of focal length and size of the imaging sensor define if a lens falls in any of the three broad categories: wide-angle, standard, and long focus lenses. All of them have their specific uses and create specific effects (such as depth of field, perspective distortion *etc*.). Often, a standard or longer focal length lens is used to minimise most geometric deformations.

For standard photography of the reflected visible radiation, daylight can be used. However, since even diffuse materials have some geometric sensitivity to lighting, the best results can be achieved using studio lighting with soft boxes, diffusing umbrellas and other light modifiers.

1.3.2.2 Applications

Colour plays a very important role in our daily life. It fascinates artists as it adds enormously to aesthetic appreciation and can invoke feelings, thoughts and emotions. Colour also interests scientists, as scientific imaging needs to be able to accurately capture colour. However, colour is only important when imaging something in the visible range. Since the colour information is coded in three wide channels by the DSC, visible imaging is by default metameric. The advantages of this approach are pragmatic: three channels are often considered sufficient for colour production while the approach is inexpensive, noise is minimised as well as the data volume.[14] The challenge now is to link the RGB values produced by the camera to the colour perceived by the human eye.

This is far from easy, as colour reproduction is device-dependent. For instance, if the same image is viewed on two different monitors, one will most likely look at two different colour renditions. This means that the same RGB triplet will be translated into a different physical colour and that cross-media reproductions become challenging. Luckily, the science of *colorimetry* offers several solutions to acquire quite accurate colours that can be faithfully reproduced on several devices. Therefore, the acquisition and reproduction devices need to be calibrated to a set of standard settings and characterised to link their own colour representation (device-dependency) to a device-independent colour representation such as CIE L*a*b* or CIE XYZ. The latter colour spaces mathematically describe how a colour is perceived by a human observer when viewed under a certain standardised illuminant. When this link is established (often in the form of an ICC profile) more or less accurate colour acquisition and cross-media colour reproduction become possible.[41,42] During the years, a large variety of image viewing conditions have been standardised, while many colour management tools—such as the ColorChecker® Digital SG target (Figure 1.7)—are currently available for device characterisation. However, these tools require some experience with colorimetry, while the whole process is still not completely full-proof since the

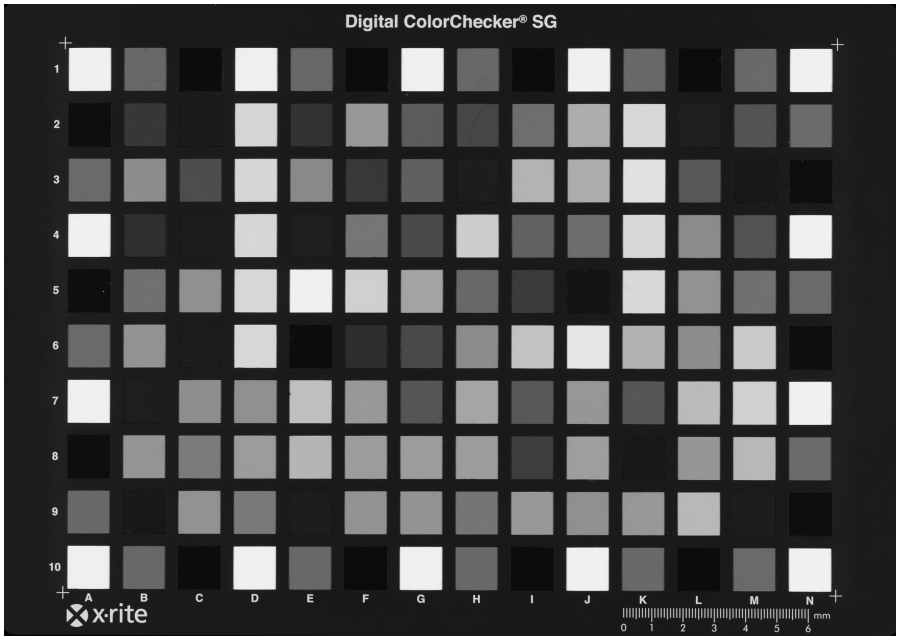

Figure 1.7 The X-Rite ColorChecker® Digital SG target often used to characterise digital cameras.

end-results largely depend on the illumination conditions.[43] In case a more accurate acquisition, processing and storage of object colour is necessary, DSCs are often changed in favour of multi- and hyperspectral imaging devices (see later), as several researchers have proven the superiority of the latter approaches.[44–46]

Besides colour, the human visual system can register very subtle differences in texture. Often, paintings are photographed with raking light to reveal the brushwork more clearly. As the angle and direction of the light source are changed, different elements can become emphasized. As long as the paint layers are not too thick, imaging with transmitted light might also be interesting to reveal incisions or earlier compositional elements.[47] When Michelangelo's David was exhaustively investigated in the beginning of the 21th century, conventional digital photography was one of the main visualisation techniques. Using raking light, direct light and natural light, the researchers tried to identify surface deterioration, surface deposits and marble imperfections.[48] Figure 1.8 shows a digital image of David's lower arm and right side of the body on which the marble imperfections (such as veins, inclusions and alveoli) are indicated. Due to the sculpting marks visible on these images, information on the tools used by Michelangelo could be inferred, as well as the order in which they were applied.[49]

Figure 1.8 Michelangelo's David restoration—conventional RGB image of the lower arm and right side of the body, with relief of marble imperfections in overlay. (Reproduced with permission from Museo Galleria dell'Accademia and CNR-ISTI, Pisa, Italy.)

1.3.3 Reflected Near-ultraviolet Photography

Reflected (sometimes called direct) NUV photography monitors the reflected NUV portion that is produced by the sun or an artificial source. By using invisible radiation, (digital) NUV photography tries to make certain features of the objects under consideration (more) distinct, because the NUV reflection will most likely differ from the characteristic visible reflectance properties. Even if they exhibit a similar reflectance in the visible spectrum, objects thus often benefit from this uncommon means of imaging (which is also the reason for animals such as honey bees to have UV vision, as NUV reflectance can reveal complex patterns that function as nectar guides).[50,51]

1.3.3.1 Tools

From all types of DSC-related imaging, NUV photography is by far the most complex. In general, one should opt for a CCD-based DSC, as these are known to be more sensitive to NUV than a CMOS imaging sensor.[35,52,53] By replacing the internal filter package with a specific clear glass or fused silica

window that largely transmits NUV, the camera becomes responsive to wavelengths about 320 nm. In the last few years, several manufacturers have provided back-illuminated (BI) or backside-illuminated (BSI) sensors, in which the sensor is not illuminated on top, but thinned by removing substrate material and illuminated from the back.[26] However, these sensors are currently not implemented in D-SLRs and thus remain largely unsuited for convenient NUV imaging, since the commercial cameras in which they are embedded do not allow changing of the lens. The latter is very important, since optical glass does generally not transmit much NUV and mostly becomes opaque to EM radiation below 350 nm. Moreover, optical cements can have a very high NUV absorption and the coatings on the lens elements might additionally decrease the NUV transmittance.[54–57] As a result, normal photographic lenses are usually impractical for NUV imaging. However, expensive expert UV lenses such as the Nikon UV-Nikkor 105 mm f/4.5 with special quartz and fluorite elements for sub-350 nm imaging do exist. Unfortunately, none of these exist in wide-angle variants. Fortunately, some older, rather exotic glass lenses still have a useful NUV transmission even below 350 nm (see Verhoeven and Schmitt[53] for a list), often due to their simple optical design with few lens elements and the absence of cemented or multi-coated elements.[58]

To cut-out the contaminating visible and NIR radiation after removal of the internal filter, a very dense visual+NIR block is of the utmost importance in digital NUV imaging. Most classic NUV band-pass filters (such as Schott UG1 and UG11, B+W 403, Kodak Wratten 18A, Nikon FF, Hoya U-330, U-340 and U-360) are Woods-Type filters that still substantially leak NIR,[54,55,58] spoiling the pure NUV picture aimed for. In contrast, a Baader Planetarium U-Filter (also called "Venus Filter") exhibits a high NUV transmission from about 320 nm to 390 nm and only leaks less than 1% NIR radiation, an amount that is far too low to perceivably contaminate the digital NUV record. This filter is therefore considered to be elementary in D-SLR NUV imaging.

Although the sun generates abundant visible radiation, it still produces a substantial amount of NUV rays that can be used for NUV imaging.[59] Only the spectral bands with shorter-wavelength UV radiant energy are largely blocked by the ozone (O_3) layer of the atmosphere and become completely useless for imaging purposes. However, studio light will be required in most imaging situations. Ideally, this studio light should only produce NUV (also called UV-A or Long Wave UV) radiation. One of the most preferable artificial NUV sources are high and low pressure Mercury vapour discharge lamps (*e.g.* the popular tubular Philips TL-D 36 W BLB SLV lamps), Xenon arcs lamps (such as those of electronic flashes), lasers and metal halide lamps (consider ref. 60 for a thorough overview). Most of them are quite compact, stable and have a constant output. Very convenient are the electronic flash lamps used for conventional visible photography. Depending on the gas mixture they contain, these flash lights can have a quite intense output in the NUV region. If this NUV is not cut-out by a yellowish lacquer layer, these sources make-up very suitable NUV imagers.[60] Commercially available

continuous Xenon lamps such as the Polilight PL500 are also very good solutions, although they are expensive and less efficient than many other sources. On the other hand, their spectral output can be pure NUV. Currently, modern NUV LEDs (light emitting diode) have become quite popular.[61,62] Although these have an output that is less intense, the spectral bandwidth of LEDs is known to be very small and often limited to about 20 nm to 40 nm.

Finally, it is important to understand that UV light is hazardous. As long as the source only emits pure NUV, the danger is minimised. However, UV-B and UV-C are completely invisible and very harmful. A photon of UV-B radiation has enough energy to cause changes in the DNA (deoxyribonucleic acid) and damage cells, causing sunburn, but also permanent severe eye damage (and blindness) and forms of skin cancer. Therefore, one should always protect the skin and eyes when using UV sources. Simple gloves and long sleeves help substantially, while special UV-blocking glasses are of the utmost importance. Finally, one should never look directly into the output beam from a UV source. To avoid damage to the object by these highly energetic photons, the exposure time should also be limited and a continuous light source turned off between exposures. Obviously, the correct exposure is determined by a test series with varying exposure settings. As exposure times can be quite long, a sturdy tripod is essential.

1.3.3.2 Results

In the fields of archaeology and cultural heritage, the use of NUV photography is more occasionally used to examine subjects not (or less) responsive to visible or NIR photographic methods. In those cases, direct NUV photography might reveal faded inks,[60,61,63–65] altered documents or engravings,[66] can aid in the study of ceramics[67] (Figure 1.9) and excavation profiles,[68] while it can also be rewarding to detect specific pigments[55,60,69] as well as traces of restoration on tapestries,[70] textiles,[69,71] paintings[55,60,72] and sculptures.[66,67] In general, it can be stated that NUV records might be quite

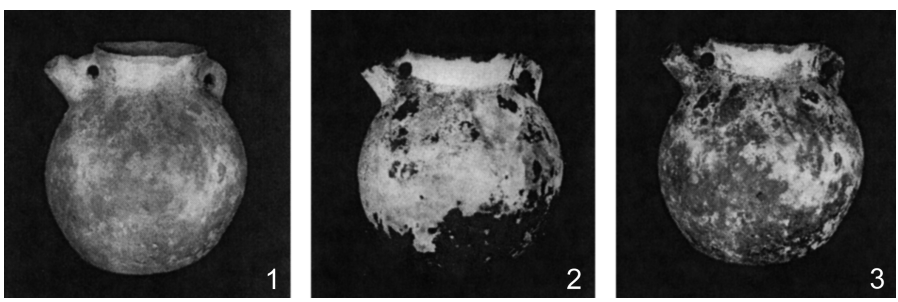

Figure 1.9 A lime-encrusted pot with covering slip, depicted by visible wavelengths (1), using NUV fluorescence (2) as well as direct NUV (3). (Reproduced with permission from ref. 67.)

difficult to read and interpret and that NUV induced fluorescence (see later) often delivers greater success.

One often overlooked advantage of direct NUV imaging is, however, the ability to resolve smaller details. Because EM radiation with short wavelengths is less prone to diffraction (*i.e.* the spreading out of waves when passing small apertures and their bending around tiny objects), the lens can focus NUV waves to a smaller point compared to visible light.[57,73,74] Moreover, smaller lens apertures (*e.g. f*/16) can easily be used in NUV imaging before any diffraction effects reduce the resolution of the final image.[53]

1.3.4 Reflected Near-infrared Photography

Since the astronomer and composer Sir Frederick William Herschel (1738–1822) discovered in 1800 the infrared (IR) portion of the electromagnetic (EM) spectrum, many scientific disciplines have become fascinated by this kind of invisible radiation. To date, there exists some misconception about NIR imaging and it gets often intermingled with heat imaging. However, these images are generated by electronic thermography, a technique based on a completely different part of the EM spectrum. Heat imaging uses the Mid and Long Wavelength IR,[51] energy given off by all real-world objects.[75] As a matter of fact, all objects with a temperature above absolute zero (0 K or −273.15 °C) emit EM radiation, but the type and amount of the latter largely depends upon the temperature of the matter. Practically, objects need to be heated to about 500 K before they start radiating in the NIR range, while a temperature of at least 800 K (*e.g.* an electric stove burner) must be attained before visible red light is emitted.[56,75] Because it is only possible to photograph the NIR portion with conventional film-based approaches or digital photo cameras, NIR photography basically visualizes the particular amounts of reflected NIR radiation (which is emitted by hot objects such as the sun and incandescent light bulbs), rather than recording the ambient temperature variation.

1.3.4.1 Tools

Until only very recently, archaeological NIR photography was performed using films whose emulsion was sensitised into the NIR range. Although generally the same cameras and radiation sources can be used as for imaging reflected visible light, digital NIR photography still features some peculiarities. First of all, it is best to remove the internal NIR-blocking filter. After replacement of this optical element with a visibly opaque filter, all visible radiation is removed before reaching the sensor (Figure 1.10). Such a modification hugely increases the DSC's sensitivity to NIR, while retaining the facility to view through the lens (impossible in the film-based approach of pure NIR imaging). In cases where the sensor is covered with a clear filter, a visible blocking filter has to be fitted onto the lens to enable pure NIR

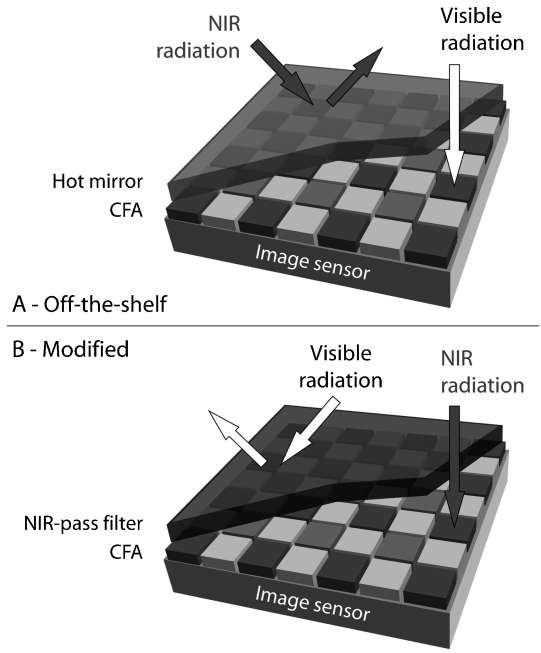

Figure 1.10 Modification of the digital imaging array by replacing the hot mirror.

photography, in which case it becomes impossible to compose the image by looking through the viewfinder.

Using a dedicated modified D-SLR, the same lenses used for the film approach can be applied, although it is still best to test whether hot spots of increased irradiance are generated by a specific camera–lens combination.[58,76] Moreover, because NIR radiation features longer wavelengths than visible light, the waves are less refracted and focus to another point which lies behind the visible focal plane. To counteract this, the lens has to be focused on an object that is closer than the actual object, a process known as short focusing. This explains why many pro and/or older lenses have a red dot/line/letter "R" indicating the NIR focus offset when focused at infinity. Newer lenses seldom display such a supplementary focusing index. Besides short focusing, a smaller diaphragm setting (*e.g. f*/8 or *f*/11)—with corresponding extended depth of field—will largely solve most of these focus errors. Too small apertures may be counterproductive, as diffraction effects start to come into play and shutter speeds become lengthy.

As illumination sources, tungsten halogen incandescent lamps, electronic flash tubes as well as continuous laser sources have been used.[77] For smaller objects, NIR emitting LEDs can also be employed. For the best results, uniform and diffuse lighting is advised.[78]

1.3.4.2 Results

Not until the 1930s were NIR sensitive emulsions relatively available, allowing photographers to practise this new technique with a certain ease and certainty. From this period onwards, the possibility to visualise an often subtle, dissimilar behaviour of materials in the NIR helped heritage researchers and archaeologists to depict certain object characteristics not (or less) apparent to the human eye. One of the research domains that benefited most from NIR photography is the investigation and decipherment of documents. Charred, dirty, worn, bleached, censored, obliterated, faded or very deteriorated documents often reveal their secrets through recording their NIR reflectance. While some inks are largely transparent, others do reflect NIR to a larger extent. Moreover, NIR often can differentiate between dyes and pigments that look indistinguishable to the human visual system.[79,80] Exploiting these spectral signature properties might bring document alterations to light or reveal the under-writing of obliterated passages in cases where the top ink is less opaque to NIR than the ink below.

Using direct NIR photography several scholars deciphered original writings on fragments of badly discoloured or charred papyri and paper manuscripts.[81–86] Famous, also, is the work of the Arab photographer Najib Anton Albina, who used reflected NIR photography in the 1950s to retrieve information from the Dead Sea scroll fragments.[87] The results achieved by Coremans[88] even proved NIR photography to reveal writings and drawings underneath encrustations (Figure 1.11) or a patina. By differentiating between the NIR reflectance and/or transmittance of the particular pigments, dyes and materials used, NIR photography also furnishes a useful means for the examination of fabrics.[67] In this way, Coremans detected tapestry restoration.[88] Baldia and Jakes even incorporated NIR photography in a complete range of photographic methods for non-destructive research of archaeological textiles.[71]

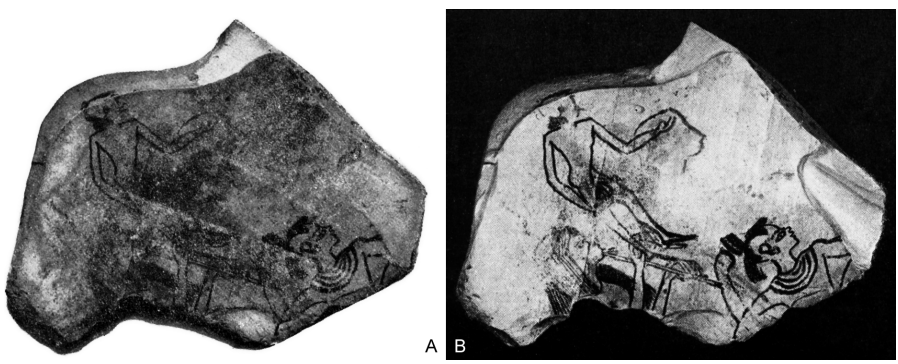

Figure 1.11 (A) Panchromatic and (B) reflected NIR photograph of the same artefact. (Reproduced from ref. 88.)

The same principles hold for the investigation of all kinds of paintings: on canvas, rock, wood or glass. Marshack utilised NIR photography in some French caves to get a deeper insight into the employed pigment and the dating of the Cro-Magnon man's cave art.[89] Besides, NIR imaging has also been demonstrated several times to be indispensable in the detection of painted forgeries, proving the authenticity and examining the fake or altered state of the art work,[90,91] as the latter might reveal information which the technique of IR reflectography (see later) is unable to unveil.[92] Canvas paintings or paper sometimes also benefits from NIR transmission lighting, in which the amount of transmitted radiation is recorded.[93]

In several studies, NIR reflected radiation has been taken into account to detect forms of tattooing on human remains that were naturally or artificially mummified.[94,95] Traces of pigments can also be found on ceramics and plaster, in which case photography by NIR can help enormously in the study of *tituli picti* (painted inscriptions), decoration *etc*. Used in combination with radiography, Milanesi demonstrated the benefit of NIR photography in dating and classifying prehistoric and protohistoric pottery fragments.[96]

Although NIR photography thus clearly proves to be a very successful method for many applications (see Gibson[97] for many other examples), reflected SWIR radiation often enables the visualization of certain features (such as the underdrawing of paintings) even better than NIR imaging as longer IR wavelengths have an increased penetration depth. This was the main reason for the development and application of SWIR reflectography (see later).

1.3.5 Fluorescence Photography

Besides imaging the reflected portions of the incident wavelengths (often called *direct or reflectance photography*), NUV, visible and NIR radiation can be used to excite EM radiation of a wavelength longer than the incident wavelengths. This type of photography is called *fluorescence photography*. Although its application is mainly restricted to the forensic field, the very strong fluorescence of particular minerals and pigments makes this type of photography worthwhile in certain archaeological and heritage case studies. Fluorescence is a specific type of *photoluminescence*: a general term for the spontaneous emission of new radiation by an object after absorbing photons. All luminescence phenomena described here are called fluorescence or *immediate luminescence*, as the emission occurs immediately after absorption the higher energy optical radiation. Delayed emission is called *phosphorescence*. As can be seen in the glow-in-the-dark toys, phosphorescence slowly fades out within seconds or up to a few hours. This is not the case with fluorescence, which only lasts during illumination.[98]

In general, three types of fluorescence photography exist: UV-induced, visible-induced and NIR-induced fluorescence. In general, these fluorescence phenomena will be imaged in the visible, NIR and SWIR spectral region

respectively (see Figure 1.12). As a result, fluorescence phenomena can be described by the radiation falling on the object or the energy emitted by the object. This situation leads to a very inconsistent terminology in which NUV fluorescence was used to denote NUV-induced fluorescence in the visible region and NIR fluorescence used for fluorescence created in the NIR region.[99] Using the terminology proposed here removes this confusion. To completely rule out any misconception, one could mention both the incident and emitted type of radiation such as NUV|visible fluorescence or visible|NIR fluorescence (Figure 1.12).

1.3.5.1 Tools

Although the requirements of the equipment are a bit more stringent compared to direct photography, the techniques and equipment involved are still fairly straightforward. Good fluorescence imaging involves a monochromatic or filtered source that does not radiate in the sensitivity range of the imager, while the latter has to block the spectral wavelength range of the source to purely record the re-radiated fluorescence. In practice, this constrains two different filters to successful fluorescence photography: firstly, an appropriate *exciter/excitation filter* must be placed over the light source to make sure the latter only emits the appropriate radiation. As an example, visible-induced NIR fluorescence photography generally uses a blue/green pass filter to prevent the output of any infrared photons (obviously, the same can be accomplished with a monochromatic source such as LEDs). Secondly, a *barrier filter* on the lens must make sure that only the fluorescence is recorded and not the much more intense portion of reflected incident radiation. In our example, a visibly-opaque NIR-pass filter has to be used to make sure only the NIR excited photons are captured, hence excluding any reflected visible light.[100] When possible, it is best to use barrier filters of the interference type, as they are better at rejecting unwanted wavelengths and therefore might deliver higher quality images than results obtained with pigment-based filters.[101]

Obviously, all kinds of fluorescence photography should be executed in a completely darkened room except for the excitation source. To enable NUV-induced fluorescence, filtered Xenon flash lamps that block any visible output can be used.[60] However, one needs to understand that it is best to have a continuous pure NUV source for preliminary observation of any NUV-induced visible fluorescent, as this can be impossibly assessed during the short flash duration. Certainly for fluorescence photography, LED solutions are very practical as their spectral output is very pure. The same considerations hold for visible and NIR-induced fluorescence. Obviously, both benefit from a LED or even laser approach, but generally speaking the same light sources can be used as for reflectance photography (*e.g.* xenon flash lamps and incandescent bulbs). Whatever excitation source is applied, it is of the utmost importance to verify that any longer-wavelength radiation is blocked.

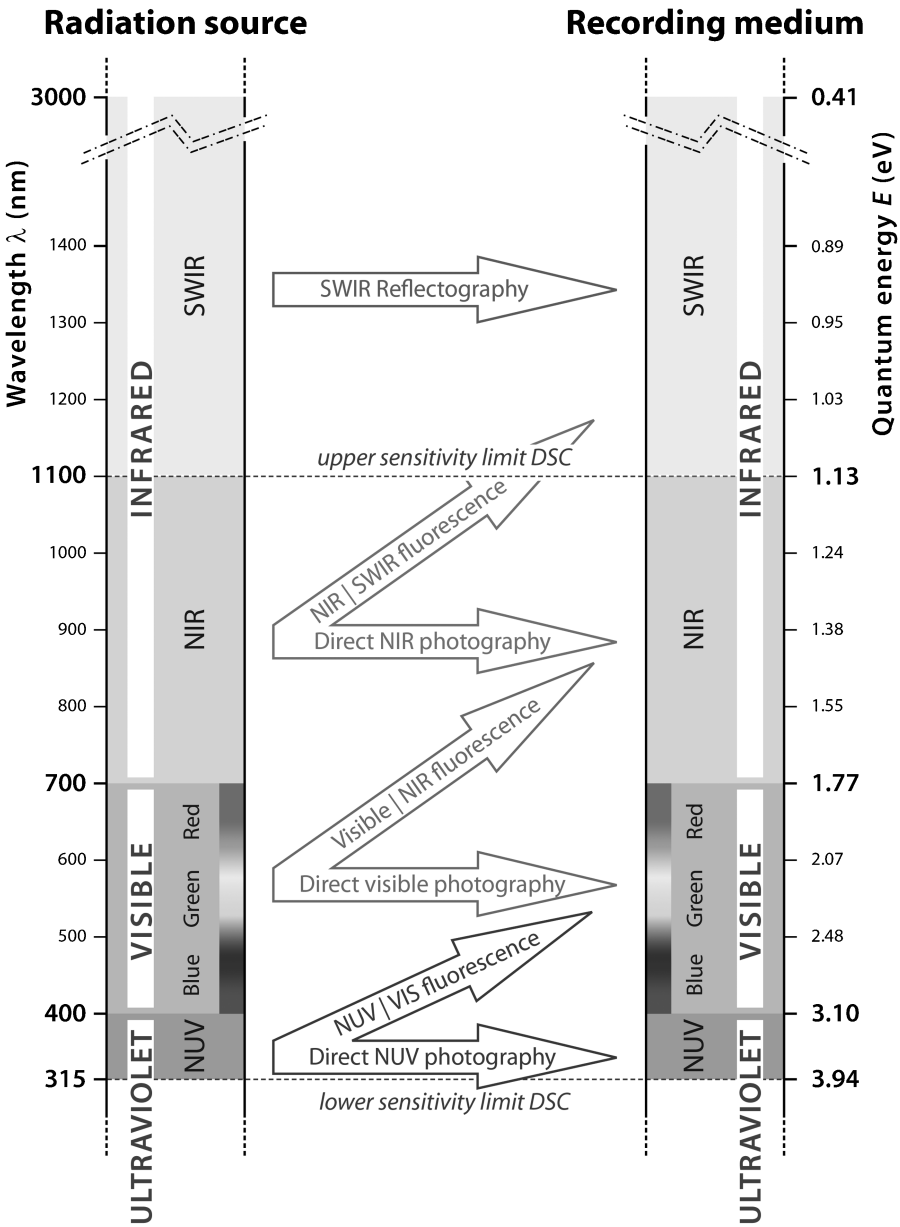

Figure 1.12 Overview of some non-invasive optical imaging methods described in this chapter.

Since NUV, visible and NIR-induced fluorescence can be imaged in the visible or NIR domain, conventional imaging equipment for direct photography can be used. One must only verify that neither the anti-reflection

coatings of the lens nor the barrier filter itself fluoresce. Evidently, the exposure determination for any kind of fluorescence must be done by trial-and-error.

1.3.5.2 Applications

Although most substances do not fluorescence,[98] several organic and some inorganic materials do exhibit fluorescence, such as organic dyes, chlorophyll, mineral oils, some glasses, and sweat.[7] As dissimilar materials might show a similar fluorescence and equal minerals of various deposits can exhibit a different fluorescence, the identification of materials based on fluorescence is very unreliable.[60,102]

The most common form of fluorescence applied is NUV-induced, which is based on the recording of the spontaneously emitted visible or NIR radiation.[103] The best known examples are the pieces of clothing with brightening agents that start to fluoresce white when walking along the "black lights" of a disco. In heritage research, fluorescence imaging has been applied mostly on paintings. Generally, pigments in paintings do not benefit from NUV-induced fluorescence photography, as most NUV is absorbed in the top layer. This, however, offers possibilities to look at the preservation state of a painting and its varnish layer, which often represents itself by a bluish to greenish fluorescence. Later additions such as over-paintings or retouches are often tracked by the darker spots in this fluorescence[47,98,102] (Figure 13B), although one must bear in mind that these additions can also start to fluoresce after some time and hence a perfectly uniform fluorescence is anything but a reliable indication of a perfect preservation state.[60] In these cases, one should also use direct NIR or SWIR imaging, visible-induced NIR fluorescence (Figure 13C), microscopic examination and X-ray examinations (see later).

Besides canvas paintings, NUV-induced fluorescence can be used to look at pigments in wall paintings and water-colour paintings or the investigation of dyed textiles. Fluorescence by NUV can also reveal (dyed) varnish layers on gilded part of wooden sculpture or metal sculptures. Additionally, it is applied to verify traces of paint on sculptures or ceramics. A very well-known application is to read deteriorated text on manuscripts. Iron gall inks absorb NUV quite well, while the paper background fluoresces under NUV illumination. Broadband visible imaging can pick up the fluorescence and significantly improve the documents' legibility. Examples are given in the work of Smith and Norman[104] or more recently in the research by Montani *et al.*[105] and Easton *et al.*[61]

In accordance with principles of NUV-induced fluorescence, visible-induced fluorescence photography records radiation emitted by the subject under study mostly in the NIR region (although the red part of the visible region is also possible). However, an object can also emit NIR radiation around 1000 nm while being illuminated with shorter, more energetic NIR wavelengths ranging from 750 nm to 850 nm. Even NUV-induced NIR fluorescence is possible and

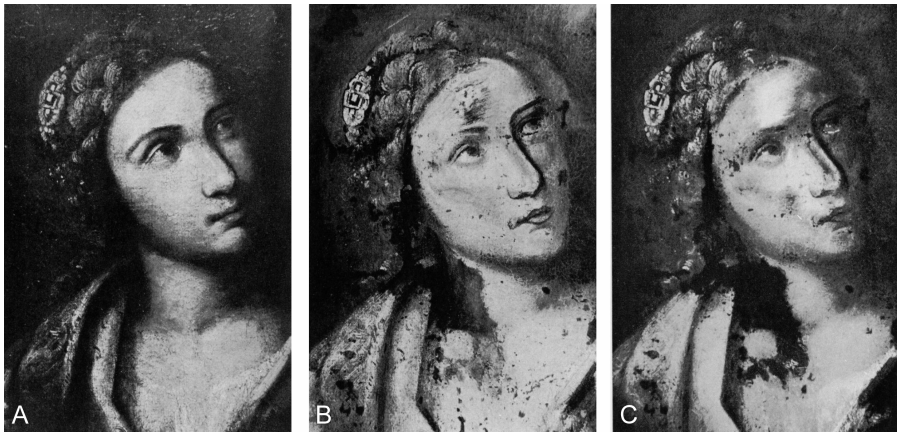

Figure 1.13 Panchromatic (A), NUV|VIS fluorescence (B) and VIS|NIR fluorescence. Both fluorescence records reveal the restored areas clearly. (Reproduced from ref. 99.)

was applied to disclose some of Vindolanda's wooden Roman writing tablets.[106] In most cases, however, fluorescence in the NIR is stimulated by blue-green visible light. Since it is known that materials such as leather, minerals, wood, natural resins and dyes can exhibit visible-induced NIR fluorescence,[78] the technique has also been applied in cultural heritage imaging to a limited extent and can be used to examine the fake or altered state of the canvas. An older but still relevant overview of fluorescence in the NIR region was published by Bridgman and Gibson[99]. A more recent article describes how intense visible|NIR fluorescence allows the mapping of Egyptian Blue.[107]

1.4 Uncovering Underdrawings: SWIR Reflectography

1.4.1 Principles

Infrared reflectgraphy (IRR) is to date the most widespread non-destructive technique to image the underdrawings of paintings (see Bomford[108] for many examples). It has a long tradition of assisting art historians and restorers, since the Dutch physicist J. R. J. van Asperen De Boer developed the technique in the late 1960s.[109–111] More specifically, van Asperen de Boer found out that most paints are best penetrated by short-wavelength infrared (SWIR) radiation that peaks around 2 μm (2000 nm) with a maximum threshold around 2.7 μm, after which oils and proteins in the paints and varnishes start to absorb.[111]

Since 2 μm-SWIR radiation maximally penetrates the paint layers, the paint is said to be transparent for this type of radiation. When a suited SWIR source is illuminating a painting, its produced EM waves will penetrate the varnish layer and thin paint film, after which they are partially reflected by the preparatory layer or absorbed by the black pigment of the possible

underdrawing on top of this ground layer. As a result, the upper paint layers themselves are not recorded, only the underlying layers reveal themselves by dissimilar absorption and reflection of the SWIR energy.[112] It thus becomes possible to get information on the deeper paint layers or even record the initial stages of the painting: graphite composition lines and underdrawings sketched in sepia or with black chalk and charcoal (Figure 1.14). The end-result of this imaging process is denoted an *IR reflectogram*. Despite the fact that the Dutch pioneer clearly distinguished an NIR photograph from an IR reflectogram,[109,111] the latter term started to lose its specific meaning. Nowadays, IRR is used for infrared reflectance imaging from the NIR to SWIR region (*e.g.* Bertani and Consolandi[82] or Walmsley *et al.*[113]). To honour the contribution of van Asperen de Boer and clearly distinguish between imaging in the NIR and SWIR region, it is deemed more appropriate to use the terms NIR photography/imaging as opposed to SWIR imaging or (SW)IR reflectography. Accordingly, their products can be called an NIR image or IR reflectogram. For those that adhere to the term IR reflectogram, the specific type can be stated: *NIR* or *SWIR* reflectogram.

1.4.2 Tools

To produce his SWIR reflectograms, Van Asperen de Boer initially used a lead-sulfide (PbS) detector with a normal tungsten filament lamp.[109,110] From 1969 onwards, he started to obtain reflectograms with a low-cost vidicon system.[111,114] Due to the limited resolving power of the vidicon systems, close-up images with quite some overlap had to be acquired. In a second stage, those images were printed and manually assembled into a mosaic representing the

Figure 1.14 Detail of a sixteenth-century pane painting shown by Van Asperen de Boer to illustrate the possibility of IR reflectography. From left to right: a conventional greyscale photograph, an NIR photograph and an IR reflectogram. (Reproduced from ref. 109.)

complete painting. In a later stage, the vidicon cameras were attached to frame-grabber boards installed in a computer. In this way, the vidicon camera's output was grabbed and all individual images could be digitally mosaicked.[82]

Van Asperen de Boer was aware that the degree of paint penetration depends on the paint itself, the thickness of the paint and also the exact wavelengths used. His idea that an optimal detection system should have a peak response at 2 μm had, however, some flaws. Many common drawing inks such as iron gall and sepia later proved to become completely invisible in these wavelengths,[115] while Walmsley *et al.*[113] clearly showed that the optimum visualisation of the underdrawing is determined by the specific combination of paint and underdrawing material. Consequently, other imaging solutions needed to be found that could not only overcome the limited spatial resolving power of the vidicon technology and its extremely low spectral sensitivity around 2 μm, but also allowed more targeted imaging in different portions of the SWIR region. According to the unique underdrawing/pigment combinations, Walmsley *et al.*[113] identified several optimised imaging bands in the NIR-SWIR region. As a result, InGaAS sensors are currently applied in NIR and SWIR reflectography as they have an extended spectral responsivity, which mean they can be equipped with particular optical filters to image very specific wavebands in the NIR-SWIR region. Moreover, their sensitivity and resolving power is many factors better than what could be obtained with the vidicon technology.[116]

For both types of reflectography, conventional lenses can be used as the absorption of most glass elements typically occurs around between 2.5 μm and 4.2 μm.[56,117] Since the subject needs to be illuminated by SWIR energy, tungsten halogen incandescent lamps and continuous laser sources can be used.

The whole imaging unit is often put on rails, allowing precise positioning of the camera in front of the painting while acquiring juxtaposable close-up images and avoiding any rotation of the optical axis (as this would complicate the procedure in which all individual close-ups are mosaicked). The problem when imaging an area in many different parts is that the illumination of the imaged area must be extremely uniform to yield a good mosaic without abrupt tone changes due to illumination non-uniformity. Irrespective of the illumination quality, all the individual tiles need to undergo some necessary image processing to get the best representation possible. Moreover, only the portion of the lens that is almost distortion-free should be used for imaging, as any deformation will hamper an accurate mosaicking of the many (tens to often hundreds or even thousands) of small image tiles (see Figure 1.15). A drawback of SWIR reflectography (and also NIR reflectography) is that the data acquisition might be very time consuming when details of large paintings have to be shot (often using scaffolding) and stitched afterwards. Finally, it needs to be said that the painting should get as minimal incident radiation as possible, as it is well known that it causes ageing processes in binding media

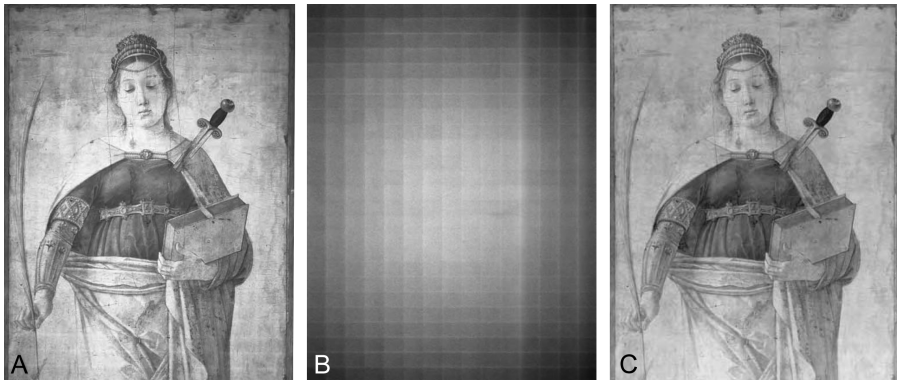

Figure 1.15 (A) Part of the uncorrected reflectogram of *S. Giustina de' Borromei* by Giovanni Bellini; (B) images of a uniform grey panel used to correct for illumination differences; (C) corrected version of (A) using (B). (Reproduced with permission from ref. 82.)

and pigments.[77] However, this type of radiation is far less harmful than NUV energy.

1.4.3 Results

The application turned out to be so valuable for art historians that IRR became an independent research field. The data obtained are applied to identify the materials and techniques used for sketching and to study how the sketching techniques evolved through time. When a certain underdrawing technique is very well known, it can even help to identify the original author of a painting or attribute it to a certain "school". Besides underdrawings, SWIR reflectography can be very valuable for studying cracks, the canvas state, deeper paint layers, hidden signatures, dates, inscriptions and *pentimenti*. *Pentimenti* (singular *pentimento*) are alterations in paintings: from slight alterations in the figures to the displacements of complete figures. Although they might still be visible by careful inspection of the paint, it is often only the underdrawing that reveals the original composition of the artists and how this was changed in the final painted version.[47,82]

Since the inks conventionally used to write on papyri absorb IR very well, SWIR reflectography can also be used to study this type of document.[118] Although it has been shown that standard NIR photography can reveal the characters of discoloured papyri, their state (*e.g.* carbonised papyri) often merits a high-resolution SWIR reflectogram as the ink still absorbs much SWIR, and thus retains its contrast with the rest of the papyrus and yields better results compared to a NIR photograph.[82] The same reasoning holds for paintings. NIR photography can indeed reveal (partly) the underdrawings of paintings that are predominately in white, brown, and red hues, but when painting areas with greens and blues are encountered, SWIR is needed as these

pigments are opaque to NIR radiation.[111,119] Finally, Falcone *et al.*[120] showed that reflectography can also be useful in reconstructing plaster inscriptions wiped off by mechanical abrasion.

1.5 Spectral Imaging

1.5.1 Principles

Theoretically, one can speak of multispectral imaging as soon as more than one spectral band is taken into account. However, the practical threshold is often four channels (*e.g.* Bianco *et al.*[43], Fairchild *et al.*[14]), since three spectral bands are by default acquired by a DSC and the human visual system and are insufficient to overcome metameric imaging. Hence, multi-spectral imaging is often considered to extend the human visual systems and DSCs traditional trichromatic RGB approach. Its application therefore generally relies on a bulkier, more expensive and less widespread hardware setup.

Hyperspectral imaging is an even more demanding technique, as it captures the reflectance spectrum of the object under study in a multitude of contiguous, small spectral channels. Compared to a multispectral sensor which yields images in several spectral bands of about 50–100 nm wide, hyperspectral sensors have a *higher spectral resolution* (often about 10 nm wide bands) and capture more and (nearly) contiguous spectra. Although the borderline between multi- and hyperspectral imaging is rather discipline dependent, ten is often taken as a threshold (*e.g.* Shrestha *et al.*[121]). In other words: tens to hundreds of many small bands of EM radiant energy are captured per pixel location. Just as with conventional D-SLRs or multi-spectral imaging, the technique is *non-invasive* and the end product a spectrally-varying stack of spatially co-registered two-dimensional reflectance images. Through a combination of all spectral data acquired from a particular spatial location, every individual pixel of the final image holds the complete reflectance spectrum (known as the *spectral signature*) of the material that was sampled at that specific location (see Figure 1.4). Since this spectral signature can be obtained for every pixel in the image, the hyperspectral technique is also known as imaging spectroscopy (spectroscopy being the study of interaction between radiant energy and matter). Here, no further distinction will be made between multi- and hyperspectral imaging and the process of capturing, processing, displaying and interpreting images with a high number of spectral channels is from now on denoted *spectral imaging*.[14] We just have to remember that the amount of spectral bands and their bandwidth can vary. In cultural heritage-related colour imaging applications, spectral images can vary from four to five broad image channels up to 40 narrow spectral bands. Obviously, more and smaller spectral channels have the potential to digitise such a spectral signature better,[122] although mathematical techniques exist to estimate the spectral signature out of only a few spectral bands.

Due to its working principles with more and smaller bands, spectral imaging captures sufficient data to separate a signal into the portion contributed by the reflection and the portion contributed by the illumination, thus enabling the estimation of quantitative spectral information such as spectral radiance, transmittance and reflectance from a medium. Therefore, the spectral reflectance function of individual objects can be captured and distinguished. Besides, spectral imaging is also attractive as it less prone to metamerism and very accurate colour information can be obtained when compared to traditional RGB imaging. Together, these two properties provide the main reasons for using a spectral system.

The drawbacks of spectral imaging revolve around the quantity of data that are gathered.[13] In addition, the acquisition of data in small spectral bands makes the imaging process more noise prone, a problem that is much less apparent with the broad channels of metameric imaging. Finally, a non-standard, customised infrastructure is essential, whereas 3-channel imaging can choose from a wide variety of industry-standardised tools for the capture, processing, and reproduction of the data.

1.5.2 Tools

Spectral imaging has been executed using a wide variety of hardware configurations. Most of these systems were custom-made prototypes for individual research purposes, while others have been produced commercially (*e.g.* Art-Innovation[123]). In most cases, a cooled or uncooled high-performance industrial camera (sometimes denoted as machine vision imager) interfaced to a computer is used. To overcome the restriction of monochrome (*i.e.* greyscale) imaging, spectroscopic capabilities are made possible by selecting various narrow or broad spectral bands with optical filters, prism-grating-prisms (PgP) and electronically tuneable elements like acousto-optic (AOTF) and liquid-crystal tunable filters (LQTF). These distinct solutions to filter or separate the incoming wavelengths have also distinct drawbacks and advantages.[25,43,124] Besides filtering the incoming radiation, it is also possible to filter the radiation source.[125]

Since most of these systems are incapable of capturing scenes in motion, one-shot systems have been proposed as well.[126,127]. A recent and very interesting approach is the one-shot system solution by Shrestha *et al.*[121]. By employing a commercial digital stereo camera and a pair of readily available optical filters, a cheap system could be assembled to acquire multi-spectral data in a practical and fast way, while additionally offering 3D stereo imagery. Such systems might have the potential to expand the usage of multispectral imaging, as most equipment has so far only been affordable for the most resourceful institutions.

The radiation source should be free from strong emission lines and bright enough that the exposure time can be minimised.[128,129] Hence the use of halogen lamps.[122] To view, pre- and post-process the huge amounts of data,

dedicated software is needed. Deriving the actual spectral data from the acquired output requires a major amount of signal processing and differs for the two existing spectral approaches based on narrowband and broadband sensors. A good overview of the general mathematics behind broadband and narrowband spectral imaging is given in Novati *et al.*[37]. Besides, mosaicking of the individual images is needed whenever a high resolution is essential or large objects have to be imaged. Often, the processing software also operates the whole imaging system. Depending on the aim of the imaging and hardware applied, this software enables the coregistration of individual images, the reconstruction of an accurate colour image, reduces the dimensionality of the data (often by a principal component analysis or PCA), clusters or distinguishes pixels based on their spectral characteristics and identifies material from their spectral signatures.

1.5.3 Applications

Initially, imaging spectroscopy was used to identify minerals from space.[130] In the last two decades, many new (ground-based) applications have arisen and spectral imaging is now also included in the fields of archaeology and art conservation. As a spectral imaging system directly assesses the spectral signature of objects irrespective of illumination, this per-pixel spectral information can be used to render the object for any given observer or viewing condition.[43,131] As such, a spectral image is device independent. In the field of painting conservation, this characteristic is often exploited. Simulating dissimilar light sources might be interesting to see how the colours of a painting were perceived under different illuminants such as daylight and candlelight (see Figure 1.16). Because any observer or illumination specific rendering should be discounted for a reliable assessment of an artefact, spectral images also constitute essential information for research on monitoring and restoring heritage objects, predicting their appearance after cleaning, reconstructing faded pigments and assess damage by transportation.[125]

Spectral imaging makes it also possible to distinguish the materials comprising the various objects in the scene that were imaged (remember, higher spectral resolutions will simplify this process as they capture distinct spectral features more faithfully). By comparing the spectral response of a region against the spectral response of known features (*e.g.* pigments), possible matches can be deduced.[112,132] This allows researchers not only to identify the pigments, but also to spatially map their distribution, opening up many interesting areas for painting research. Padfield *et al.*[133] could, for instance, visualise the dissimilar distribution of the yellow ochre and lead–tin yellow pigment at the surface of the painting and in the underpaint. Besides paintings, pigment mapping has been applied to study and reveal written documents and look at old conservation treatments. Although NIR, NUV and fluorescence photography proved to be very valid tools for making unreadable carbon-black text on leather, papyrus, pottery sherds and clay tablets discernible

Figure 1.16 Daylight (A) and candlelight (B) rendering of *Heads of Angels*. (Reproduced with permission from ref. 131.)

again, multispectral imaging of those subjects has shown the extra amount of information that can often be retrieved.[61,118] The key is to use very small spectral bands, as broadband imagery loses spectral selectivity and spectrally unique features—such as very faint traces of ink that only reflect in a small waveband—might get lost due to mixing with neighbouring wavelengths. Those interested in more archaeological and art conservation examples are referred to the works of Kubik[128] and Liang.[124]

Although spectral imaging is not restricted to the visible and near-infrared spectrum, this VNIR waveband is dominating its application since one of the main aims for imaging spectroscopy in cultural heritage is a nearly flawless colour treatment: from the acquisition, processing, and storing to reproducing images with a very high colour quality.[43,134] Although it might seem strange to use NIR information in accurate colour reproduction, sufficient NIR data proved to be important since colours such as cobalt blue have important NIR information which has to be taken into account.[40] In the past two decades, many studies have been conducted to determine the amount of (theoretical and real) filters needed for accurate colour imaging. Although the aim was always to create digital image archives with very high colour accuracy, there is so far no agreement on the minimum amount of spectral bands to achieve this: four spectral dimensions were proposed by Eem *et al.*,[135] five to seven by

Maloney,[136] six by Lenz *et al.*,[137] Parkkinen *et al.*[138] claim that eight is essential while Hardeberg[139] calculated eighteen basic spectral channels. Besides the test set of known reflectances being used, these discrepancies are mainly explained by the dissimilar methods and thresholds applied to assess the colour reconstruction error. In an attempt to remedy this and quantify the influence of image noise, Connah *et al.*[140] derived various optimized sensor configurations and simulated how they could recover the reflectance function in the presence of quantization and shot noise. In the end, they found that the colour reconstruction error in a typical imaging situation with some shot noise could be minimised by using eight to thirteen spectral bands, the exact number depending on the object imaged. These numbers indicate maximum values, since noise prevents a further decrease in colour error when using more sensors (although most colour errors are already virtually eliminated). This characteristic of spectral imaging can be exploited by storing spectral images as master copies in cultural archives and digital museums; not only for printed reproductions in books, brochures, catalogues and as posters, but also for accurate display of artefacts that can not be showcased.[37] In general, it is safe to state that spectral imaging professionalised and revolutionised the non-invasive imaging techniques explained in the previous sections.

1.6 X-Ray Radiography

1.6.1 Principles

Although X-rays do not belong to the optical band of EM radiation, they have been used for over a century as a diagnostic tool in cultural heritage imaging since they enable the non-destructive internal visualisation of objects. Whereas all previous techniques could be classified as non-invasive surface techniques, X-ray imaging is considered a *bulk technique* since it allows the internal structure of the material to be imaged.[141] In most cases, X-ray imaging is still treated as a non-invasive technique because the object under study does not need to be physically penetrated to execute this imaging method. However, the technique can be considered invasive on an atomic scale, since high-energy photons are passing through the sample.

The existence of Röntgen radiation was revealed by the German physicist Wilhelm Conrad Röntgen in 1895,[142] who named this unknown type of radiation X-rays, and was credited for this discovery with the Nobel Price for Physics in 1901. With wavelengths between 0.01 nm to 10 nm, the X-ray region is characterised by very energetic photons with energies between 124 keV to 124 eV. The complete X-ray regime is often split into two observational regions, referred to as the *soft X-rays* and *hard X-ray band*. Conventionally, the soft region spans the 0.10 nm to 10 nm region (12.4 keV to 124 eV) and hard X-rays have an energy level beyond 12.4 keV per photon. Hence, hard X-rays have the highest penetration abilities. Since they all surpass the threshold of 10 eV, all Röntgen rays are considered to be *ionising radiation*, which means they

are composed of photons with enough energy to remove an electron from an atom and making it an *ion*.

X-Rays can be used to yield visualisations in different dimensions. Although one-dimensional X-ray imaging is possible (called a *gauge measurement*), most X-ray imaging yields data in two (2D) and three (3D) spatial dimensions. 2D X-ray imaging is the most widely employed imaging method in artefact visualisation and medicine.[143] It can be used to create a *projection radiograph* of an artefact: a visualisation of the complete artefact by its projection on a two-dimensional sensor. This working principle is identical to all photographic methods outlined before, although a *projection radiograph* is not created by reflected radiation but by transmitted radiation. Because of its common use, projectional radiography is generally referred to as simply *radiography* or *X-ray radiography* and its result denoted a *radiograph* or *Röntgenograph* (Figure 1.17B). When translating a three-dimensional feature onto a 2D radiograph, only lateral information is preserved. Since the loss of artefact depth information can complicate the accurate reading of a radiograph, *X-ray computed tomography* or simply *computed tomography* (CT) was invented.[143,144] Using image processing algorithms, a 3D X-ray representation of the artefact can be calculated out of a large series of 2D projection radiographs acquired at different orientations to the object (see Figure 17C). Although CT is a very interesting method that surpasses certain inherent drawbacks of 2D radiographs, this chapter will only focus on radiography and its applications.

Even though the X-ray application field is a difficult and broad one, the basic principles of X-ray imaging are conceptually fairly simple. The visualisation of an object's density distribution is enabled by differential absorption properties.[141] This absorption of X-rays is primarily dependent on the energy and amount of X-rays and the electron concentration per unit volume of the material, which can be roughly estimated by the atomic number, Z, of the atom.[145] Lead (Pb), for instance, has 82 protons and electrons per atom ($Z = 82$) and therefore absorbs X-rays very well.[146] Many materials are only averagely absorbing: paper, wood, ceramics, organic material, rock, light metals, paintings.[141] The clinical importance of radiography stems from the fact that human soft tissue has a transmittance to X-rays seven times as high as bone,[147] since human flesh is composed of light elements such as oxygen ($Z = 8$) and carbon ($Z = 6$). Besides the distribution of matter, the differential thickness of the imaged object also produces an absorption contrast.[148]

1.6.2 Tools

To create an X-ray radiograph, a generator, artefact and detector are needed. The X-ray generator such as an X-ray tube produces X-rays, which are filtered to reduce scatter and noise. This filtered radiation, sometimes called the *primary beam*, is directed towards the object under study. In the object, the primary beam gets *attenuated* by differential absorption of the X-rays. What

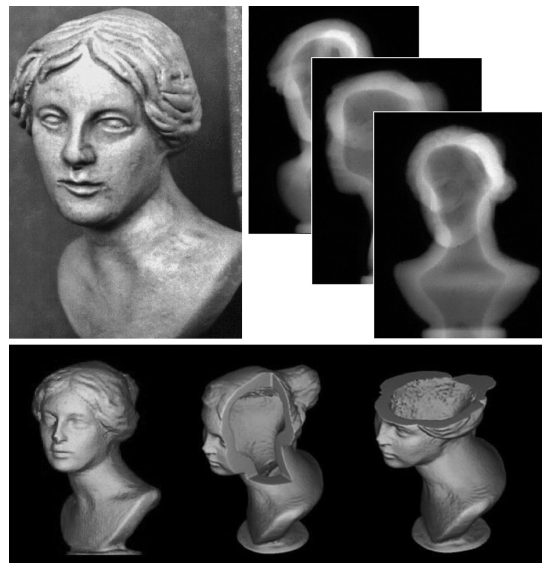

Figure 1.17 (A) Small clay head (copy of a find in Pompeii, Italy); (B) X-ray radiographies of (A); (C) 3D CT of (A). (Reproduced with permission from ref. 149.)

remains of the incoming Röntgen radiation after attenuation emerges on the other side of the object. This *remnant bean* exposes the X-ray detector, which can vary from a sheet of dedicated photographic film or X-ray sensitive phosphorescent plate to one of the many direct and indirect digital detectors.[149–151] In the first case, the latent image on the film is chemically processed to a two-dimensional *radiograph*, while the second method yields a *digital radiograph*.[144] Areas of the object that highly attenuate the incoming X-rays expose the detector to a minimal extent. During conversion of the negative image to a positive radiograph (*cf*. conventional photographic negative), these zones will be rendered very light. Conversely, X-ray transmitting parts expose the sensor maximally and are depicted very dark on the final greyscale radiograph. Since nearly everyone has some experience with an X-ray examination, try to remember this principle by visualising an X-ray radiograph of the human body (bone, tooth, chest): dense and highly absorptive bone structures are always processed as white, while soft tissue is rendered in dark grey tones.[144] As radiographs record the transmitted X-rays, they are really just the shadows of the artefacts that are imaged. Hence, they are also called *shadowgraphs*.

As one might recall from an X-ray examination, the instrumentation geometry can be changed and adapted according to the size of the object, the required resolution of the end-result, the type of detector and the source of radiation.[149–151] Although the working principle of X-ray sources is beyond the scope of this chapter, it is useful to know that research, archaeology and

conservation applications nowadays widely use a specialised source of X-rays called *synchrotron radiation*. The advantages of these sources are a much higher X-ray output compared to the conventional X-ray tubes, high polarization and a better collimation (*i.e.* lower divergence) of the radiation.[152] Finally, it needs to be said that X-rays are highly energetic so imaging them brings with it some health and safety procedures. In general, one can say that the time to X-ray exposure should be as short as possible, the distance between the X-ray source and radiographer as large as possible and the physical shielding as good as possible.[143]

1.6.3 Applications

Although the technique only became widely applied after WWI, X-ray imaging had already been applied to study paintings in the late 1890s and the beginning of the 20th century.[153] Currently, most objects routinely analysed using X-ray radiography are paintings, for which it almost became a standard technique. The popularity of X-ray imaging can be explained by the additional information it made available to art historians and conservators. Since the image is formed by differential attenuation of the X-rays passing through the object, the absorbency patterns on an X-radiograph can disclose information on the paint pigments. Pigments such as lead white are relatively opaque in X-radiographs as they contain elements of a high atomic number, whereas cadmium-based pigments ($Z = 48$) such as yellows or reds appear quite transparent.[47] Besides, X-ray radiography discloses data on the painting's entire three-dimensional structure such as wooden support, canvas weave and areas with paint loss.[133] Additionally, one could trace paint forgeries or assess the painting's condition and applied methods, which might in their turn be useful to distinguish different artists and previous compositions, all because the X-rays reveal information about the paint layers itself. Due to the fact that extremely short wavelengths are used, very high magnifications with an extreme spatial resolution are also possible.[145] Often, the X-ray sensitive film is in direct contact with the surface of the painting, allowing for accurate measurements on the exact 1 : 1 Röntgen rendering.[47] Because the dimensions of the film are limited (typically 300 mm $\times$ 400 mm) a mosaic of individually exposed frames is needed to completely image the entire painting surface, a process that is hugely simplified after digitising each X-ray image by a purpose-built or commercially available scanner. In the case of digital X-ray radiography imaging, the film is commonly replaced with a scintillator that converts the incoming X-rays of the remnant beam to visible light that can be detected by a conventional CCD.

Since it is relatively cheap, fast, non-destructive and can be applied on a wide variety of averagely-absorbing materials, X-ray imaging has been used a lot to examine the internal features of archaeological objects such as mummified bodies[154,155] and closed recipients.[156] Besides showing the content of these vessels, X-ray radiography can also be used to acquire details on the

manufacturing of ceramics and several studies have shown that it is a valuable tool for understanding forming techniques of ancient vessels. Carr showed that radiographs could help in a more accurate interpretation of ceramics and sorting ambiguous vessels.[157] Pierret *et al.* applied X-radiography to extract a density and porosity distribution across different vessels.[158] Using over 100 custom-made vessels in controlled experiments, Berg could deduce many new insights on wheel-thrown and wheel-shaped pots and assess the impact of surface treatments and secondary forming techniques on inclusion established during primary forming.[159] For more examples of X-radiography in an archaeological context, Malainey[160] can be consulted.

1.7 Conclusions

Since the invention of photography, a wide variety of approaches and means have enabled the non-invasive visualization and examination of our cultural heritage for a variety of reasons and applications. The basic concepts, technologies, and application of various non-destructive, low- and high-cost, single band, multi- and hyperspectral imaging solutions currently applied in the field of archaeology, museology, art conservation and art history have been briefly presented. First of all, it was made clear that the observed digital result depends upon the interaction of two components (radiation source and medium) whose result finally interacts with the receptor. In addition, it has been shown that metameric imaging is by default applied in almost every imaging area, certainly when working with conventional RGB DSCs. Additionally, the advantages of non-visible imaging, fluorescence visualisations, spectral imaging and X-ray radiography have been explored.

The examples provided here show that each of the specific techniques has the potential to yield particular information on the artefact studied. However, these methods really start to shine when a variety of techniques can be applied on the same object, since no single technique will serve as one universal method for artefact visualisation. When the results are integrated properly, all possible methods complement one another and form a very powerful visualisation combination for all kinds of objects that can gain an enormous amount of useful information.

Because all optical techniques described here can be considered as non-invasive techniques that can easily be applied *in-situ*, the risk to damage or alteration of the heritage object during handling and transportation is substantially minimised. X-Ray radiography forms a bit an exception to this. However, given the usefulness of its application and the fragility of many objects, some very large museums have also acquired their own X-ray equipment. This can be considered very positive and indicates that a better understanding of our cultural heritage is only possible when the technological suspicion of art historians, conservators and archaeologists further decreases.

References

1. *Digital heritage: Applying digital imaging to cultural heritage*, ed. L. MacDonald, Elsevier, Amsterdam, 2006.
2. J. C. Slater and N. H. Frank, *Electromagnetism*, Dover Publications, New York, 1969.
3. G. Waldman, *Introduction to light: The physics of light, vision, and color*, Dover Publications, Mineola, N.Y, 2002.
4. J. S. Walker, *Physics*, Pearson Education, Upper Saddle River, N.J., 2004.
5. J. M. Palmer and B. G. Grant, *The art of radiometry*, SPIE Press, Bellingham, Washington D. C., 2010.
6. Y. Ohno, in *Handbook of Optoelectronics*, ed. J. P. Dakin and R. G. Brown, Taylor & Francis, Boca Raton, 2006, p. 287.
7. G. Gauglitz and J. P. Dakin, in *Handbook of Optoelectronics*, ed. J. P. Dakin and R. G. Brown, Taylor & Francis, Boca Raton, 2006, p. 1399.
8. B. Hapke, *Theory of reflectance and emittance spectroscopy*, Cambridge University Press, Cambridge, 1993.
9. M. Livingstone, *Vision and art: The biology of seeing*, Abrams, New York, 2002.
10. B. A. Wandell, *Foundations of vision*, Sinauer Associates, Massachusetts, 1995.
11. A. Stockman and L. T. Sharpe, *Vision Research*, 2000, **40**, 1711.
12. P.-C. Hung, in *Image sensors and signal processing for digital still cameras*, ed. J. Nakamura, Taylor & Francis, Boca Raton, 2006, p. 205.
13. F. König and P. G. Herzog, in *PICS 1999: Proceedings of the Conference on Image Processing, Image Quality and Image Capture Systems (PICS-99)*, 1999, p. 163.
14. M. D. Fairchild, M. R. Rosen and G. M. Johnson, *Spectral and Metameric Color Imaging*, RIT-MCSL Technical Report, 2001.
15. A. Rogalski and Z. Bielecki, in *Handbook of Optoelectronics*, ed. J. P. Dakin and R. G. Brown, Taylor & Francis, Boca Raton, 2006, p. 73.
16. W. S. Boyle and G. E. Smith, *Bell Syst. Technol. J.*, 1970, **49**, 587.
17. P. Magnan, *Nucl. Instrum. Methods Phys. Res., Sect. A*, 2003, **504**(1–3), 199.
18. E. R. Fossum, in *Proceedings of the 1997 Multimedia Technology & Applications Conference (MTAC97)*, 1997, p. 1.
19. S. K. Mendis, S. E. Kemeny and E. R. Fossum, *IEEE International Electron Devices Meeting (IEDM)*, 1993, 583.
20. http://www.dalsa.com/corp/markets/ccd_vs_cmos.aspx (last accessed 03/01/2012).
21. J. R. Janesick, *Fundamentals of scientific charge-coupled devices*, SPIE, Bellingham, WA, 2001.
22. H. Kume, in *Handbook of Optoelectronics*, ed. J. P. Dakin and R. G. Brown, Taylor & Francis, Boca Raton, 2006, p. 413.
23. http://www.sensorsinc.com/GaAs.html (last accessed November 2011).
24. M. Nelson, M. Bush, M. Skrutskie, S. Kanneganti, C. Park and O. Fox, in *High Energy, Optical, and Infrared Detectors for Astronomy II*, ed. D. A. Dorn and A. D. Holland, 2006, p. 62761R–627610R.

25. C. Fisher and I. Kakoulli, *Rev. Conserv.*, 2006, **7**, 3.
26. O. Nixon, *Adv. Imaging*, 2008, **23**(2), 24.
27. Visions Connection, Trax/UV Back Illuminated^{TM} – World's First Back-Illuminated UV CMOS Camera, San Diego, 2011.
28. R. Berry and J. Burnell, *The handbook of astronomical image processing*, Willmann-Bell, Richmond, VA, 2005.
29. G. J. J. Verhoeven, P. Smet, D. Poelman and F. Vermeulen, *IEEE Trans. Geosci. Remote Sensing*, 2009, **47**(10), 3456.
30. G. C. Holst, *CCD arrays, cameras, and displays*, JCD Pub; SPIE Optical Engineering, Winter Park FL, Bellingham, Wash., USA, 1998.
31. H. T. Hytti, in *Image Quality and System Performance III*, ed. L. C. Cui and Y. Miyake, SPIE, 2005.
32. Y. Reibel, M. Jung, M. Bouhifd, B. Cunin and C. Draman, *Eur. Phys. J.: Appl. Phys.*, 2003, **21**(1), 75.
33. K. Toyoda, in *Image sensors and signal processing for digital still cameras*, ed. J. Nakamura, Taylor & Francis, Boca Raton, 2006, p 1.
34. J. Nakamura, in *Image sensors and signal processing for digital still cameras*, ed. J. Nakamura, Taylor & Francis, Boca Raton, 2006, p 55.
35. D. Har, Y. Son and S. Lee, in *Sensors and Camera Systems for Scientific, Industrial, and Digital Photography Applications V*, ed. M. M. Blouke, N. Sampat and R. J. Motta, IS&T - SPIE, Bellingham, 2004, p 276.
36. G. J. J. Verhoeven, *J. Archaeol. Sci.*, 2008, **35**(12), 3087.
37. G. Novati, P. Pellegri and R. Schettini, *International Journal on Digital Libraries*, 2005, **5**(3), 167.
38. P.-C. Hung, in *Camera and Input Scanner Systems*, ed. W. Chang and J. R. Milch, SPIE, 1991, p 164.
39. R. S. Berns, *J. Imaging Sci. Technol.*, 2001, **45**(4), 305.
40. F. H. Imai, S. Quan, M. R. Rosen and R. S. Berns, in *Proceedings of the Third International Conference on Multispectral Color Science*, ed. M. Hauta-Kasari, J. Hiltunen and J. Vanhanen, 2001.
41. R. S. Berns, Billmeyer and Saltzman's principles of color technology, Wiley, New York, 2000.
42. R. W. Hunt, *The reproduction of colour*, John Wiley & Sons, Chichester, 2004.
43. S. Bianco, A. Colombo, F. Gasparini and R. Schettini, in *Digital Imaging for Cultural Heritage Preservation: Analysis, Restoration, and Reconstruction of Ancient Artworks*, ed. F. Stanco, S. Battiato and G. Gallo, CRC Press, Boca Raton, 2012, p 183.
44. R. S. Berns, L. A. Taplin, F. H. Imai, E. A. Day and D. C. Day, in *Eleventh Color Imaging Conference: Color Science and Engineering Systems, Technologies, and Applications*, 2003, p 149.
45. F. M. P. B. Ferreira, P. T. Fiadeiro, V. M. N. de Almeida, M. J. T. Pereira, J. Bernardo and S. M. C. Nascimento, in *CGIV 2006 – Third European Conference on Color in Graphics, Imaging and Vision*, The Society for Imaging Science and Technology, 2006, p 350.

46. M. Yamaguchi, H. Haneishi and N. Ohyama, *J. Imaging Sci. Technol.*, 2008, **52**(1), 010201-010201-15.
47. H. Cooper and R. Spronk, *Mondrian: the transatlantic paintings*, Yale University Press; Harvard University Art Museums, New Haven, Cambridge, Mass, 2001.
48. A. Parronchi, in *Exploring David. Diagnostic Tests and State of Conservation*, ed. S. Bracci, F. Falletti, M. Matteini and R. Scopigno, Giunti - Firenze MVSEI, Florence-Milan, 2004, p 100.
49. P. Giovannini, in *Exploring David. Diagnostic Tests and State of Conservation*, ed. S. Bracci, F. Falletti, M. Matteini and R. Scopigno, Giunti - Firenze MVSEI, Florence-Milan, 2004, p 104.
50. A. G. Dyer, *Aust. J. Bot.*, 1996, **44**, 473.
51. A. Richards, *Alien vision: Exploring the electromagnetic spectrum with imaging technology*, SPIE Press, Bellingham, WA, 2001.
52. http://photographyoftheinvisibleworld.blogspot.com/2007/09/canon-dslrs-for-uv.html (last accessed November 2008).
53. G. J. J. Verhoeven and K. D. Schmitt, *J. Archaeol. Sci.*, 2010, **37**(4), 833.
54. C. R. Arnold, P. J. Rolls and J. C. J. Stewart, *Applied photography*, Focal Press, London, New York, 1971.
55. F. Mairinger, in *Non-destructive microanalysis of cultural heritage materials*, ed. K. H. A. Janssens and R. van Grieken, Elsevier, Amsterdam, London, 2004, p 15.
56. S. F. Ray, *Scientific photography and applied imaging*, Focal Press, Oxford, 1999.
57. S. F. Ray, *Applied photographic optics: Lenses and optical systems for photography, film, video, electronic and digital imaging*, Focal Press, Oxford, 2002.
58. www.naturfotograf.com/UV_IR_rev00.html (last accessed July 2008).
59. L. R. Koller, *Ultraviolet Radiation*, Wiley, New York, 1965.
60. F. Mairinger, in *Radiation in Art and Archeometry*, ed. D. C. Creagh and D. A. Bradley, Elsevier Science, Amsterdam, 2000, p 20.
61. R. L. Easton, Jr., W. A. Christens-Barry and K. T. Knox, *Commentationes Humanarum Litterarum*, 2011, **129**, 5.
62. http://photographyoftheinvisibleworld.blogspot.com/2007/10/nichia-365nm-uv-led-based-uv.html.
63. A. A. Blaker, *The South African Archaeological Bulletin*, 1968, **23**(89), 24.
64. S. K. Matthews, *Photography in Archaeology and Art*, John Baker, London, 1968.
65. D. G. Pearce, *The Digging Stick*, 2003, **20**(3), 8.
66. Eastman Kodak Company, *Infrared and Ultraviolet Photography*, Eastman Kodak Company, Rochester, N.Y, 1961.
67. P. G. Dorrell, *Photography in archaeology and conservation*, Cambridge University Press, Cambridge, 1994.
68. J. T. Dorwin, *Am. Antiq.*, 1967, **32**(1), 105.

69. J. van Santen, *Ultravioletlampen als analytisch en fotografisch hulpmiddel*, Focus, Bloemendaal, 1946.
70. P. R. Lichtmann, *Oriental Rug Review*, 1995, **15**(6), 28.
71. C. M. Baldia and K. A. Jakes, *J. Archaeol. Sci.*, 2007, **34**(4), 519.
72. H. Marceau, *Proc. Am. Philos. Soc.*, 1953, **97**(6), 686.
73. R. S. Longhurst, *Geometrical and physical optics*, Longmans, London, 1967.
74. H. D. Young, R. A. Freedman and F. W. Sears, *Sears and Zemansky's university physics: with Modern Physics*, Pearson/Addison Wesley, San Francisco, 2004.
75. R. Barnes, *Sci. Technol. Cult. Heritage*, 1963, **140**(3569), 870.
76. http://www.naturfotograf.com/lens_surv.html (last accessed 12_03_2011).
77. C. Dietz, G. Catanzariti and A. J. Martínez, *e-conservation*, 2011, **18**, 32.
78. F. Mairinger, in *Radiation in Art and Archeometry*, ed. D. C. Creagh and D. A. Bradley, Elsevier Science, Amsterdam, 2000, p 40.
79. A. Brüning, *Archiv Kriminol.*, 1939, **104**(Heft 1–2), 19.
80. K. Ross, *Zeiss-Nachr.*, 1933, **4**, 19.
81. I. Andorlini, G. Menci, D. Bertani, M. Cetica and P. Poggi, *Sci. Technol. Cult. Heritage*, 1993, **2**, 115.
82. D. Bertani and L. Consolandi, in *Digital heritage: Applying digital imaging to cultural heritage*, ed. L. MacDonald, Elsevier, Amsterdam, 2006, p 211.
83. D. M. Chabries, S. W. Booras and G. H. Bearman, *Antiquity*, 2003, **77**(296), 359.
84. D. L., The British Journal of Photography, 1933, **80**(3812), 311.
85. T.-P. Nguyen, S. Bouvet, A. Komenda and B. Dumont, *Restaurator*, 2008, **29**, 155.
86. D. Obbink, *Literary and Linguistic Computing*, 1997, **12**(3), 159.
87. L. H. Schiffman, *Reclaiming the Dead Sea Scrolls: The history of Judaism, the background of Christianity, the lost library of Qumran*, Doubleday, New York, 1995.
88. P. Coremans, *Bulletin des musées royaux d'art et d'histoire*, 1938, **10**(4), 87.
89. A. Marshack, *National Geographic*, 1975, **147**(1), 64.
90. A. Aldrovandi, D. Bertani, M. Cetica, M. Matteini, A. Moles, P. Poggi and P. Tiano, *Stud. Conserv.*, 1988, **33**(3), 154.
91. R. A. Lyon, *Technical Studies in the Field of the Fine Arts*, 1934, **2**, 203.
92. M. Gargano, N. Ludwig and G. Poldi, *Infrared Phys. Technol.*, 2007, **49**(3), 249.
93. L. Lazzarini, *Notizie da Palazzo Albani*, 1974, **2–3**, 38.
94. A. Alvrus, D. Wright and C. F. Merbs, *J. Archaeol. Sci.*, 2001, **28**(4), 395.
95. G. S. Smith and M. R. Zimmerman, *Am. Antiq.*, 1975, **40**(4), 433.
96. Q. Milanesi, *Rivista di Scienze Preistoriche*, 1963, **18**, 287.
97. H. L. Gibson, *Photography by Infrared: Its Principles and Applications*, Wiley, New York, 1978.
98. E. R. de La Rie, *Stud. Conserv.*, 1982, **27**(1), 1.

99. C. Bridgman and H. L. Gibson, *Stud. Conserv.*, 1963, **8**(3), 77.
100. H. L. Gibson, *Med. Biol. Illus.*, 1962, **12**, 155.
101. L. Bravo Pereira, *Int. J. Conserv. Sci.*, 2010, **1**(3), 161.
102. E. R. de La Rie, *Stud. Conserv.*, 1982, **27**(3), 102.
103. G. H. Schenk, *Absorption of Light and Ultraviolet Radiation: Fluorescence and Phosphorescence Emission.: An Introduction with Experiments*, Allyn and Bacon, Boston, 1973.
104. A. Smith and F. Norman, *London Medieval Studies*, 1938, **1, Part 2**, 179.
105. I. Montani, E. Sapin, A. Pahud and P. Margot, *J. Cult. Heritage*, 2012, **13**(2), 226.
106. A. Rutherford, *Med. Biol. Illustr.*, 1977, **27**, 35.
107. G. Verri, in *The Nebamun wall paintings: Conservation, scientific analysis and display at the British Museum*, ed. A. Middleton and K. Uprichard, Archetype Publications; In Association with the British Museum, London, 2008.
108. *Underdrawings in Renaissance paintings: Art in the making*, ed. D. Bomford, National Gallery Company, London, 2002.
109. J. R. J. van Asperen de Boer, *Stud. Conserv.*, 1966, **11**(1), 45.
110. J. R. J. van Asperen de Boer, *Appl. Opt*, 1968, 7(9), 1711.
111. J. R. J. van Asperen de Boer, *Stud. Conserv.*, 1969, **14**(3), 96.
112. P. Kubelka and F. Munk, *Z. Tech. Phys.*, 1931, **12**, 593.
113. E. Walmsley, C. Metger, J. K. Delaney and C. Fletcher, *Stud. Conserv.*, 1994, **39**(4), 217.
114. J. R. J. van Asperen de Boer, *Stud. Conserv.*, 1974, **19**(2), 97.
115. A. Burmester and F. Bayerer, *Stud. Conserv.*, 1993, **38**(3), 145.
116. J. R. J. van Asperen de Boer, in *Recent developments in the technical examination of early Netherlandish painting: Methodology, limitations perspectives*, ed. M. Faries and R. Spronk, Brepols, Turnhout, 2003, p 57.
117. http://www.schott.com/advanced_optics/german/download/schott_tie-35_transmittance_october_2005_en.pdf (last accessed December 2011).
118. G. H. Bearman and S. I. Spiro, *The Biblical Archaeologist*, 1996, **59**(1), 56.
119. M. Faries, in *Scientific examination of art: Modern techniques in conservation and analysis*, ed. National Academy Of Sciences, National Academies Press, Washington, DC, 2005, p. 87.
120. L. Falcone, F. Bloisi, V. Califano, M. Pagano and L. Vicari, *J. Phys. D: Appl. Phys*, 2007, **40**(18), 5547.
121. R. Shrestha, A. Mansouri and J. Y. Hardeberg, *EURASIP J. Adv. Signal Process.*, 2011, **57**, 1.
122. A. Pelagotti, A. del Mastio, A. de Rosa and A. Piva, *IEEE Signal Process. Mag.*, 2008, **25**(4), 27.
123. http://www.art-innovation.nl/ (last accessed December 2011).
124. H. Liang, *Appl. Phys. A*, 2012, **106**(2), 309.
125. K. Martinez, J. Cupitt, D. Saunders and R. Pillay, *Proc. IEEE*, 2002, **90**(1), 28.
126. http://www.fluxdata.com/ (last accessed December 2011).

127. K. Ohsawa, T. Ajito, Y. Komiya, H. Fukuda, H. Haneishi, M. Yamaguchi and N. Ohyama, *J. Imaging Sci. Technol.*, 2004, **48**(2), 85.
128. M. Kubik, in *Physical techniques in the study of art, archaeology and cultural heritage: Volume 2*, ed. D. C. Creagh and D. A. Bradley, Elsevier, Amsterdam, 2007, p 199.
129. M. Tsuchida, T. Kawanishi and J. Yamato, *NTT Communication Science Laboratories*, 2010, **8**(11), 243–0198.
130. A. F. Goetz, *Remote Sensing of Environment*, 2009, **113**, S5.
131. H. Liang, D. Saunders, J. Cupitt and C. Lahanier, in *Conservation of Ancient Sites on the Silk Road: Proceedings of the Second International Conference on the Conservation of Grotto Sites*, ed. N. Agnew, The Getty Conservation Institute, Los Angeles, 2010, p. 267.
132. H. Liang, K. Keita, B. Peric and T. Vajzovic, in *Proceedings of OSAV'2008. The 2nd International Topical Meeting on Optical Sensing and Artificial Vision*, 2008, p. 33.
133. J. Padfield, D. Saunders, J. Cupitt and R. Atkinson, *National Gallery Techn. Bull.*, 2002(23), 62.
134. B. Hill, in *Proceedings of Color Imaging: Device-Independent Color, Color Hardcopy, and Graphic Arts V*, ed. R. Eschbach and G. G. Marcu, SPIE, 2000, p 2.
135. J. K. Eem, H. D. Shin and S. O. Park, in *Proceedings of the Second IS&T/SID Color Imaging Conference: Color science, systems, and applications*, IS&T, Springfield, Va, 1994, p 127.
136. L. T. Maloney, *J. Opt. Soc. Am. A*, 1986, **3**(10), 1673.
137. R. Lenz, M. Österberg, J. Hiltunen, T. Jaaskelainen and J. Parkkinen, *J. Opt. Soc. Am. A*, 1996, **13**(7), 1315.
138. J. P. S. Parkkinen, J. Hallikainen and T. Jaaskelainen, *J. Opt. Soc. Am. A*, 1989, **6**(2), 318.
139. J. Y. Hardeberg, in *CGIV 2002. Proceedings of the First European Conference on Color in Graphics, Imaging and Vision, Society for Imaging Science and Technology*, 2002, p 480.
140. D. Connah, A. Alsam and J. Y. Hardeberg, *J. Imaging Sci. Technol*, 2006, **50**(1), 45.
141. G. Artioli, *Scientific methods and cultural heritage: An introduction to the application of materials science to archaeometry and conservation science*, Oxford University Press, Oxford, New York, 2010.
142. W. C. Röntgen, *Nature*, 189653, (274–276).
143. H. E. Jr. Martz, C. M. Logan and P. J. Shull, in *Nondestructive evaluation: Theory, techniques, and applications*, ed. P. J. Shull, Marcel Dekker, New York - Basel, 2002, p. 447.
144. P. H. Carter, *Imaging Sci.*, Blackwell Science, Oxford, 2006.
145. C. A. MacDonald, in *Handbook of optics: Volume V. Atmospheric Optics, Modulators, Fiber Optics, X-Ray and Neutron Optics*, ed. M. Bass, C. M. DeCusatis, J. M. Enoch, V. Lakshminarayanan, G. Li, C. A.

MacDonald, V. N. Mahajan and E. W. van Stryland, McGraw-Hill, New York, 2010, p. 26.5–26.12.
146. E. M. Gullikson, in *Handbook of optics: Volume V. Atmospheric Optics, Modulators, Fiber Optics, X-Ray and Neutron Optics*, ed. M. Bass, C. M. DeCusatis, J. M. Enoch, V. Lakshminarayanan, G. Li, C. A. MacDonald, V. N. Mahajan and E. W. van Stryland, McGraw-Hill, New York, 2010, p. 36.1–36.10.
147. G. Saxby, *The science of imaging: An introduction*, CRC Press, Boca Raton, 2011.
148. D. Pfeiffer, in *Handbook of optics: Volume V. Atmospheric Optics, Modulators, Fiber Optics, X-Ray and Neutron Optics*, ed. M. Bass, C. M. DeCusatis, J. M. Enoch, V. Lakshminarayanan, G. Li, C. A. MacDonald, V. N. Mahajan and E. W. van Stryland, McGraw-Hill, New York, 2010, p. 31.1–31.11.
149. F. Casali, in *Physical techniques in the study of art, archaeology and cultural heritage: Volume 1*, ed. D. A. Bradley and D. C. Creagh, Elsevier, Amsterdam, 2006, p. 41.
150. A. Couture, in *Handbook of optics: Volume V. Atmospheric Optics, Modulators, Fiber Optics, X-Ray and Neutron Optics*, ed. M. Bass, C. M. DeCusatis, J. M. Enoch, V. Lakshminarayanan, G. Li, C. A. MacDonald, V. N. Mahajan and E. W. van Stryland, McGraw-Hill, New York, 2010, p. 61.1–61.9.
151. W. Gibson and P. Siddons, in *Handbook of optics: Volume V. Atmospheric Optics, Modulators, Fiber Optics, X-Ray and Neutron Optics*, ed. M. Bass, C. M. DeCusatis, J. M. Enoch, V. Lakshminarayanan, G. Li, C. A. MacDonald, V. N. Mahajan and E. W. van Stryland, McGraw-Hill, New York, 2010, p. 60.3–60.11.
152. D. C. Creagh, in *Physical techniques in the study of art, archaeology and cultural heritage: Volume 2*, ed. D. C. Creagh and D. A. Bradley, Elsevier, Amsterdam, 2007, p. 1.
153. A. Burroughs, *Art criticism from a laboratory*, Little, Brown and Company, Boston, 1938.
154. *Paleoradiology: Imaging mummies and fossils*, ed. R. K. Chhem and D. R. Brothwell, Springer, Berlin, Heidelberg, New York, 2008.
155. J. E. Harris and E. F. Wente, *An X-ray atlas of the royal mummies*, University of Chicago Press, Chicago, 1980.
156. P. Martinetto, E. Dooryhee, M. Anne, J. Talabot, G. Tsoucaris and P. Walter, *ESRF Experimental Reports*, 1999, **32**(4), 10.
157. C. Carr, *Am. Antiq.*, 1993, **58**(1), 96.
158. A. Pierret, C. Moran and L.-M. Bresson, *J. Archaeol. Sci.*, 1996, **23**(3), 419.
159. I. Berg, *J. Archaeol. Sci.*, 2008, **35**(5), 1177.
160. M. E. Malainey, *A consumer's guide to archaeological science: Analytical techniques*, Springer, New York, 2011.